EDF R&D

DEPARTEMENT LABORATOIRE NATIONAL D'HYDRAULIQUE ET ENVIRONNEMENT
GROUPE OUVRAGES D'EAU ET ENVIRONNEMENT

6, QUAI WATIER
F-78401 CHATOU CEDEX

TEL : 33 1 30 87 72 52
FAX : 33 1 30 87 80 86

DEPARTEMENT CERTIFIE AFAQ ISO 9001/2000

March 2004

DAVIES A.G. *, VILLARET C.

Modelling the effect of wave-induced ripples on littoral sand transport

HP-75/03/029/A

*University of Wales Bangor, School of Ocean Sciences, Menai Bridge, Anglesey, LL59 5AB, U.K.

Related Documents :

Abstract: This report is a compilation of two papers dealing with the numerical modelling of sand transport in the coastal zone.

The first paper, untitled 'Prediction of sand transport rates by waves and currents in the coastal zone', has been presented at the Physics of Estuaries and Coastal Seas International Conference in 2001 and published in the Special Issue of the *Continental Shelf Research* (*22,* 2002). The second one, untitled 'Sediment transport modelling for coastal morphodynamics', has been presented at the *International Conference on Coastal Sediments'03* (may 2003, Florida). Here, different codes of the hydro-informatic system TELEMAC have been applied successively, in order to predict the wave-induced littoral transport.

The appendix gives a detailed description of the formulation which has been programmed in the morphodynamic module Sisyphe, in order to calculate the wave-induced ripples dimensions.

Auteurs	DAVIES A.G., VILLARET C.
Code Action	P7502R
Classement Interne	P75J25

Type de rapport	Etudes
Nombre de pages	47
Orientation dans le fonds documentaire	☐ EDF DOC (accès à tous les agents EDF) ☒ R&D DOC (accès aux seuls agents R&D) ☐ CONFIDENTIEL (accès réservé à la hiérarchie de l'entité émettrice)
Mots-clés	Transport de sédiments, houle, courant, formes de fond, rides

Indice	Auteur	Vérificateur	Approbateur
A	VILLARET Catherine signé le	GARAPON Antoine signé le	FOURNIER Jean-Christophe signé le ☑ Autorise l'exploitation de la version électronique de cette note* pour alimenter les fonds documentaires de Galaxie. * *sauf pour les notes confidentielles*.

	Destinataire	Dept	Nb		Destinataire	Dept	Nb
@	Fonds-documentaire	AGIR/CIVAP	1	@	J. Lher	CETMEF	1
	C. Villaret	EDF/LNHE	1	@	P. Sergent	CETMEF	1
@	D. Aelbrecht	EDF/LNHE	1	@	F. Sabatier	CEREGE	1
@	J.C. Fournier	EDF/LNHE	1	@	M. Provensal	CEREGE	1
@	M. Benoit	EDF/LNHE	1	@	C. Machet	LNHE	1
@	A.G. Davies	UWB	1	@	J.M. Hervouet	LNHE	1
@	A. Garapon	EDF/LNHE	1	@	C. Teisson	LNHE	1

Pré diffusion aux destinataires signalés par *	Diffusion : P pour pages de garde et contrôle, S pour pages de garde, de contrôle et de synthèse @ pour version électronique

SYNTHESE

MODELISATION DE L'EFFET DES RIDES GENEREES PAR LA HOULE SUR LE TRANSPORT LITTORAL

Ce rapport présente deux papiers concernant la modélisation du transport sédimentaire en zone littorale.

Le premier papier, intitulé 'Prediction of Sand Transport Rates by Waves and Currents in the Coastal Zone', a été publié dans un numéro spécial de la revue *Continental Shelf Research (22*, 2002). Ce papier discute la précision des méthodes qui peuvent être utilisées pour calculer le taux de transport des sédiments sous l'action combinée de la houle et du courant. Nous avons comparé les résultats obtenus entre deux modèles :

- un modèle d'ingénieur : nous avons utilisé la formule de Bijker qui a été programmée dans le code morphodynamique Sisyphe du système Télémac,
- un modèle 1DV de turbulence 'intra-wave', développé à l'UCW.

Les prédictions ont été comparées à des mesures in-situ mises à disposition par les laboratoires HR Wallingford (Maplin Sand et Boscombe Pier) et Delft Hydraulics (Egmond Beach).

Le second papier, intitulé 'Sediment Transport Modelling for Coastal Morphodynamics' a été présenté à la Conférence Internationale *Coastal Sediments'03* (mai 2003, Florida).

Différents codes du système Telemac ont été mis en oeuvre successivement pour calculer le transport littoral, dans le cas d'une plage rectiligne et uniforme:

- le code Tomawac a été utilisé pour calculer la propagation de la houle,
- le code Telemac-2d a permis de calculer le courant littoral généré par la houle,
- le code morphodynamique Sisyphe a été enfin appliqué pour calculer le transport littoral, en fonction du forçage hydrodynamique (houle et courant).

Nous présentons une étude de sensibilité des résultats obtenus par rapport au paramètre de rugosité qui dépend lui-même des dimensions des rides générées par la houle. La méthode de Wiberg et Harris (1992) a été implémentée dans Sisyphe pour calculer les dimensions des rides à l'équilibre (pour une description détaillée, se référer en annexe). Le modèle permet de reproduire la formation des rides pour des houles modérées et leur disparition dans la zone de déferlement où le transport s'effectue sur fond plat ('sheet flow'). Les rides se reforment ensuite vers le haut de plage, lorsque l'énergie de la houle a été entièrement dissipée.

Ce travail a été réalisé dans le cadre des projets européens MAST III SEDMOC No. MAS3-CT97-0115, et SANDPIT (5^{e} PCRD N° EVK3-CT-2001-00056), sur un financement partiel du Cetmef (Programme biparti).

EXECUTIVE SUMMARY

MODELLING THE EFFECT OF WAVE-INDUCED RIPPLES ON LITTORAL SAND TRANSPORT

This report is a compilation of two papers dealing with the morphological modelling of sand transport rates under the action of waves and currents.

The first paper untitled 'Prediction of Sand Transport Rates by Waves and Currents in the Coastal Zone', has been published in a special issue of the *Continental Shelf Research* (*22,* 2002). We discuss here the accuracy of two different models which can be used to predict sand transport rates :

- a turbulence intra-wave model (developed at UCW),
- an engineering model (the Bijker formula, which is implemented in Sisyphe, a morphodynamical model developed at LNHE).

Model results have been compared with data from Boscombe Pier and Maplin Sands, (HR Wallingford, UK) and data from Egmond Beach (Delft Hydraulics).

The second paper untitled 'Sediment Transport Modelling for Coastal Morphodynamics' has been presented at the International Conference on *Coastal Sediments'03* (mai 2003, Florida).

In the second paper, we present some applications using successively different codes of the Telemac hydro-informatic system to calculate the wave-induced littoral transport:

- the wave propagation code Tomawac,
- the hydrodynamic code Telemac-2d,
- the morphodynamical model Sisyphe.

Model results for the sand transport rates were shown to be highly sensitive to the choice of the bed roughness coefficient. Prediction of ripples dimensions and bed roughness parameters have been implemented in Sisyphe according to the method of Wiberg and Harris (1992) (see in the appendix, for a complete description of this method). Equilibrium ripples are predicted outside the surf zone, which are progressively washed out within the surf zone, where sediment is transported as 'sheet flow' above flat bed. Ripples are created again in the upper part of the beach after dissipation of the wave energy.

This work has been carried out as part of European Union MAST III SEDMOC Project No. MAS3-CT97-0115, and of the EU 5th Framework SANDPIT Project No. EVK3-CT-2001-00056. Partial funding from the French Ministry of Equipment (Centre d'Etudes Maritimes et Fluviales) is also acknowledged.

OUTLINE

1. Prediction of sand transport rates by waves and currents in the coastal zone

Abstract

The predictions of a sand transport research model and Bijker's (1971) engineering model are compared with data obtained in wave-current conditions at three field sites. A key element in the present study is that the bed roughness at the three sites has been estimated from predictions of the sand ripple dimensions. The comparisons between suspended sand concentrations and transport rates show that a considerable amount of uncertainty (factor ±5 or more) arises when individual predictions are compared with the measurements. However the overall bias in each set of comparisons is smaller than this, with overall agreement being within a factor of ±2 in most cases. While the results demonstrate that research models, adapted for field application, may be used to make practical sand transport computations with as much accuracy as engineering formulations, the true benefit of research models lies in the improved understanding of transport processes that they provide. This is illustrated with reference to the mechanism of grain size sorting caused by oblique incidence of waves on a current.

1.1. Introduction

One of the challenges facing coastal engineers and oceanographers is to develop improved predictive models of sand transport rates in wave and current conditions. To this end, models of widely differing complexity have been developed in recent years. These may be characterised as 'research models' that resolve the details of intra-wave sediment transport processes as a first step towards the determination of net sand transport rates, and 'engineering models' that yield the transport rate more directly by means of simplified parameterisations of, often complex, physical mechanisms.

The predictions of four typical research models were intercompared with laboratory data obtained in sheet flow conditions by Davies *et al* (1997). It was found that the models predicted net sediment transport rates beneath asymmetrical waves, and also in collinearly combined wave and current flows, to well within a factor of 2 of the measured values. In addition, cycle-mean, suspended sediment, concentration profiles were predicted to similar accuracy by most of the models. However, when a subset of these research models, including the 'TKE-model' discussed in this paper, was compared with field data at the start of the EU MAST3 SEDMOC project (1998-2001), the agreement between the models and measurements was generally unconvincing, both in respect of the net transport rate and also suspended concentrations (Van Rijn *et al*, 2001). Both quantities tended to be under-predicted substantially due, in large part, to the use of an equivalent bed roughness (k_s) more appropriate for laboratory work.

The choice of an appropriate bed roughness (k_s) is a critical step towards making realistic sediment transport predictions; for example, for plane beds, use of a (small) laboratory-derived value of k_s can lead to the prediction of much larger concentration gradients in the near-bed layer than found on site and, hence, to underprediction of suspended

concentrations and transport rates. Similar uncertainty can occur for rippled beds, though here k_s values based on laboratory work can turn out to be larger than found in the field. Since most engineering models are calibrated for field conditions, there is a tendency for their predictions to be less volatile than the predictions of research models, partly for this reason (Van Rijn *et al*, 2001).

While the primary role of research models is to provide an improved understanding of sediment transport processes, for example by allowing critical tests to be carried out on the importance of competing physical mechanisms, a secondary justification for the development of such models is that they should guide improvements in engineering formulations. The present paper aims to demonstrate initially that, provided a research model is adapted for field use, it can be used to predict sand transport rates with as much accuracy as a typical engineering model. This is not, in itself, a great advance since research models are necessarily far more difficult to implement than engineering models. However their inclusion of intra-wave processes gives them much 'added value', the most obvious example of which is their prediction of the wave-related component of the sediment flux, a phenomenon which is included in few practical formulations. This is highlighted here with reference to sediment grain size sorting on the shore face caused by flux veering.

In this paper, predictions are obtained using a turbulence-closure model based on that of Davies and Li (1997) and also Bijker's (1971, see also 1992) practical model. Since the present implementation of both models has been discussed in the companion paper of Davies and Villaret (2000) (hereafter 'DV2000'), only the most relevant features of the models are reviewed here, particularly concerning the treatment of the bed roughness for field situations. Initially, the results from both models are illustrated for a defined range of wave and current conditions, and the models are then inter-compared with data from three contrasting field sites. Finally, the 'added value' of the research model solutions is discussed with reference to flux veering.

1.2 The models

1.2.1 Bijker's (1971) sand transport model

Although Bijker's (1971) model is long established, it is still used quite widely by practising engineers due to its ready implementation and also the fact that its predictions are broadly similar to those of more recent, more complicated, practical models (see Van Rijn *et al*, 2001). The Bijker model was developed for use in general offshore, combined wave and current conditions, such as those considered later. It also has the appeal of being based on classical sediment transport concepts for the bed load and suspended load, rather than being based purely upon empirical curve fitting to transport data.

Bijker's model starts from considerations of the bed load in steady flow. The bed load transport rate (S_b) is calculated using the skin friction component of the bed shear stress based on the equivalent roughness $k_s = D_{90}$ (where 90% of the sediment by volume has grain size finer than D_{90}), and is scaled by an experimentally derived coefficient 'b' taken here as $b = 5$. In common with other practical formulations, Bijker's model takes account of the presence of ripples on the bed simply through the prescription of k_s. Specifically, the total bed shear stress is calculated using $k_s = \max(D_{90},\eta)$, in which the determination of ripple height (η) is left to the user. The associated suspended load transport rate (S_s) is based on a reference

concentration derived from S_b and implemented at height $z = k_s$. Above this level, a standard Rouse concentration profile is assumed with Rouse number $Z = W_s/(\kappa u_*)$, where u_* is the friction velocity based on the total bed shear stress, W_s is the sediment settling velocity and κ is Von Karman's constant.

For combined waves and currents, the bed shear stress is modelled by use of the quadratic friction law. As noted by DV2000, the formulation adopted by Bijker for the mean shear stress is highly non-linear, and particularly so for waves superimposed on weak currents. This has the effect of increasing the reference concentration while, at the same time, decreasing the Rouse number, with significant consequences for the predictions discussed later.

1.2.2 TKE model (based on Davies and Li, 1997)

The TKE model is a local, one-dimensional (vertical) numerical formulation, based on a One-Equation, turbulent kinetic energy closure. The model, which predicts both intra-wave and cycle-mean sediment concentrations and fluxes, has been used previously only above 'flat beds', with a bed roughness (k_s) appropriate for laboratory work. Here it has been i) adapted to allow it to be run in 'flat bed' cases with any predicted or prescribed bed roughness (k_s) and ii) extended to allow it to be run in 'rippled bed' cases. The procedure used to determine whether the bed is 'flat' or 'rippled' is outlined in the next section.

Model for 'flat' beds

The term 'flat bed' is used here to refer to 'dynamically plane' rough beds, including rippled beds of small steepness (≤ 0.12), above which momentum transfer occurs by turbulent processes (rather than organised vortex shedding). The predicted, or prescribed, roughness (k_s) of such surfaces is typically much greater than the grain roughness, taken here as $k_s' = 2.5D_{50}$, particularly in field conditions. In order to achieve a consistent description of the near-bed flow, the model formulation has been adapted by the introduction of a 'skin friction' sub-model. This (analytical) device relates the lowest computational level in the numerical turbulence-closure scheme (at height $z = z_A = k_s/30$) to the lower (skin friction) bed level at $z = z_0 = k_s'/30 = D_{50}/12$). The instantaneous (analytical) velocity profile in the near-bed layer is assumed to be logarithmic, and to be matched to the outer (numerical) logarithmic layer at a height corresponding to one half of the oscillatory boundary layer thickness.

In cases in which the bed is 'flat', the instantaneous bed load transport has been estimated using the formula of Meyer-Peter and Muller (see Li and Davies, 1996), and the bottom boundary condition for the time-varying suspended load has been taken as the reference concentration $C_b(t)$ of Engelund and Fredsre (1976). Here $C_b(t)$, defined at height $z = 2D_{50}$ and expressed as a function of the (skin friction) Shields parameter θ', has been implemented in a quasi-steady manner, moderated by the procedure of Hagatun and Eidsvik (1986) to account for sediment settling (see DV2000). The inclusion of the skin friction sub-model allows the model to be run even in 'flat bed' cases in which level z_A is greater than the height $2D_{50}$ at which $C_b(t)$ is calculated. In such situations, $C_b(t)$ is simply rescaled, using an assumed power law concentration profile with Rouse number (Z) based on the skin friction velocity, to determine the effective reference concentration at the bottom of the numerical grid at height z_A. This turns out to be a most important step in the calculation procedure. Finally,

the components of the instantaneous suspended flux in both the current and transverse directions have been corrected to allow for the additional sediment flux in the skin friction layer. For cases in which suspension is the dominant transport mode, this correction is normally less than 5% of the suspended load.

Model for 'rippled' beds

For cases involving ripples of large steepness ($\geq$0.12), the original 'flat bed' model of Davies and Li (1997) has been extended by the inclusion of a near-bed, one-dimensional, semi-analytical, sub-model. In this sub-model momentum transfer, which is dominated by the process of vortex formation and shedding, is represented by the strongly time-varying 'convective eddy viscosity' of Davies and Villaret (1999), with the sediment diffusivity in the near-bed layer being linked to this eddy viscosity. Above the near-bed vortex layer, assumed to be of thickness equal to two ripple heights, the model reverts (via matching conditions) to the standard 'flat bed' turbulence closure scheme. In cases in which the bed is 'rippled', the bottom condition for suspended sediment has been defined as a pick-up function, applied at the ripple crest level, and with mean value consistent with Nielsen's (1986) formulation. The phase of time-varying sediment entrainment is linked to the occurrence of vortex shedding from the bed. Further details about this rippled-bed sub-model will be given elsewhere.

1.3 Prediction of bed roughness and suspended sand size

If neither the bed roughness (k_s) nor the suspended grain size (D_s) is known from observation, these quantities must be predicted from the hydrodynamic inputs and grain size composition of the bed. The approaches discussed by DV2000 are summarised briefly here.

Prediction of k_s

The formulation of Wiberg and Harris (1994) for waves in isolation has been used as the starting point to calculate the heights (η) and wavelengths (λ) of the seabed ripples in any given case. These ripples are predicted to be 'orbital', 'sub-orbital' or 'anorbital', depending upon the value of the ratio d_0/D_{50} (where d_0 = orbital diameter). To allow for the superimposition of a current on the waves, the orbital diameter d_0 used in the above procedure has been replaced by αd_0, where α is given by the formula of Tanaka and Dang (1996). In particular, the waves have been treated as sinusoidal with angle of attack (φ) in the range $[0,\pi/2]$, and α ($\geq$1) has been based on the resolved component of the current in the wave direction. Subject to a maximum ripple steepness criterion (see DV2000), the bed roughness (k_s) has been determined i) in the TKE model from the rule $k_s = 25\eta(\eta/\lambda) + 5\theta'_{wc}D_{50}$, where θ'_{wc} is the peak value of Shields parameter (skin friction) in the wave-current cycle, and ii) in Bijker's model from the definition $k_s = \max(D_{90},\eta)$. It should be emphasised, that the two models, although starting with the same estimated ripple heights (η) employ rather different values for the bed roughness (k_s).

Prediction of D_s

For the TKE-model runs, the size, and hence settling velocity, of the grains in suspension has been calculated as follows. The TKE model has been run initially with $k_s = 2.5D_{50}$ to obtain the peak bed shear stress τ'_{wc} (skin friction) in the wave-current cycle and, hence, the (skin friction) friction velocity u'_{*wc}. Based on a log-normal grain size distribution curve (see Li and Davies, 1997), the largest grains in suspension (diameter D_{crit}) are assumed to have settling velocity $W_{s,crit} = 0.8u'_{*wc}$ (Fredsøe and Deigaard, 1992), this size D_{crit} being determined here using Soulsby's (1998) settling velocity formula. The median diameter D_s of the grains in suspension has then been determined, and its settling velocity $W_{s,susp}$ has been obtained by further use of Soulsby's formula. Although the number of grain size fractions in suspension has been taken here as one, the procedure may be extended to treat multiple grain fractions, for example by use of the procedure described by Li and Davies (2001). In the present single-size approach, the reference concentration has been re-scaled in proportion to the percentage (by volume) of bed material that is capable of being suspended. This correction becomes particularly important when only a very small proportion of the bottom sediment is smaller than D_{crit}.

In Bijker's model, the settling velocity has been based simply on the median diameter of the bed material, again for consistency with Bijker's formulation.

1.4 Standard model runs with predicted k_s and D_s

We present initially results for the net sand transport rate in wave-current flow that illustrate the overall behaviour of the two models. An analogous set of results was presented by DV2000, based on a set of prescribed values for bed roughness (k_s) and suspended sand size (D_s) (c.f. Van Rijn, 1993, Appendix A). Here, in contrast, k_s has been predicted for both models, and D_s has been predicted for the TKE model, using the procedures outlined earlier. The comparison involved eleven currents alone, and four waves combined with these currents at an angle of attack of $\pi/2$ in water of depth 5 m, temperature 15° and salinity. The waves, referred to hereafter as 'Waves 1 to 4', were defined respectively by their significant heights (H_s = 0.5, 1, 2 and 3 m) and peak periods (T_p = 5, 6, 7 and 8 s), and the depth-mean velocity (U_c) varied in the range 0.1 - 2 m/s. The waves were treated as purely sinusoidal, and near-bed velocity amplitudes (U_w) based on wave height H_s and period T_p were calculated using linear wave theory. The seabed sediment was assumed to comprise sand having D_{50} = 0.25 mm and D_{90} = 0.5 mm. In Table 1, the predicted values of k_s and D_s used as inputs to the TKE model are shown for the currents combined with Waves 1 and 3. All of the predicted values of k_s are considerably larger than the skin-friction value $k_s = 2.5D_{50} = 0.625$ mm. For Wave 1, the roughness varies from k_s = 0.182 m (rippled bed) to 0.0019 m (flat bed), while for Wave 3 the roughness corresponds to that of a flat bed throughout. In these flat bed cases, the sand size in suspension (D_s) is only a little smaller than D_{50} for the bed material. However, for the rougher beds beneath Wave 1, D_s becomes significantly smaller than D_{50}.

Figures 1a,b show the model results for the total sediment transport rate (Q_t). The five full lines (with symbols) show predictions of Q_t for the current alone and, successively, for the current in combination with the four waves. The effect of the waves is substantial, particularly for the smaller currents where wave stirring increases Q_t by at least an order of magnitude. Both the TKE model and Bijker's model give rise to a far less regular pattern of Q_t-curves than found in the earlier comparison based on prescribed values of k_s and D_s (see

DV2000). The present curves show some interesting features, due mainly to the behaviour of the bed roughness (k_s). For Waves 3 and 4, the bed is predicted to be plane for all values of U_c. However, for Waves 1 and 2, and also for the current alone, the bed is initially rippled, but then gradually becomes 'washed out' as the current strength increases. The resulting variations in k_s are sufficient to cause the Q_t-curves in Figure 1a to overlap. For example, when $U_c \approx 1.5$ m/s, the TKE model predicts that the addition of Waves 1 and 2 causes Q_t to decrease (due to the decrease in k_s). The addition of Wave 3 reverses this trend and, finally, the addition of Wave 4 produces the largest transport rate. Bijker's model (Figure 1b) exhibits similar behaviour for the larger currents but suggests that, for $U_c \approx 1.5$ m/s, the addition of Waves 1 and 2 has a very small effect on Q_t. For small current strengths, Bijker's model produces a fairly regular pattern of Q_t-curves, but with significantly larger transport rates than the TKE-model as soon as even small waves are added. For $U_c \leq 1$ m/s, the TKE model suggests that the transport rates for Waves 2 and 3 (rippled and plane bed, respectively) are roughly equal, while Bijker's model suggests that Wave 3 produces a somewhat larger transport rate than Wave 2.

1.5 Model comparisons with data from three field sites

Comparisons have been made with data from three field sites, chosen on account of their differing sediment sizes. Both models have been applied without additional calibration, and assuming 'equivalent sinusoidal waves' defined by their height H_s and period T_p. Although two of the sites (Boscombe Pier, Poole Bay, U.K., and Maplin Sands, Outer Thames Estuary, U.K.) were considered by DV2000, some of those earlier results are included here for comparison with results obtained at the third site (Egmond Beach, The Netherlands). The hydrodynamic conditions at the sites are summarised in Table 2, and the seabed composition and predicted sand ripple dimensions are given in Table 3. Detailed description of the data from Boscombe and Maplin are provided in Whitehouse *et al* (1997) and (1996), respectively, and details of the Egmond data are provided in Kroon (1994) and Wolf (1997).

1.5.1 Comparisons with data from Boscombe Pier and Maplin Sands

At Boscombe, long period, large waves were superimposed on relatively weak currents, at a variety of angles of wave attack. No observations were made of the roughness of the fine sand bed during the 7 tests considered. However, on the basis of the procedures outlined earlier, the roughness is predicted to have varied between low ripples and plane bed. In Figure 2 a comparison is shown between measured (pumped samples) and predicted suspended concentrations at two heights above the bed. At the lower level (0.1 m) the TKE model (Figure 2a) over-predicts the measured concentrations somewhat, while at the upper level (0.5 m) the concentration is under-predicted, and very substantially so in some tests. Although the measured concentration at the upper level may have included a fine 'wash load', the results suggest that the predicted near-bed concentration gradient is too large. The equivalent comparison for Bijker's model (Figure 2b) shows that, while the concentration is over-predicted at both heights, it is always within the factor ±10 agreement band. The concentration gradient in Bijker's model is significantly smaller than in the TKE model due to the small values of Rouse number resulting from Bijker's formulation for wave-current interaction.

At Maplin, low, short period waves were combined with relatively strong currents, over a range of angles of wave attack. No observations were made of the bedforms during the 18 tests considered here. The predicted roughness of the very fine sand bed varied between steep sand ripples and plane bed. Figures 3a,b show the predictions of the TKE and Bijker models in comparison with concentrations (pumped samples) measured at two heights (0.05 and 0.1 m). Most of the points plotted for each model fall well within the ±10 agreement band at each height. As far as the present TKE model results (Figure 3a) are concerned, the agreement between the predictions and measurements is rather better, in at least a subset of cases, than for the equivalent results for Maplin presented by DV2000. In that paper, the TKE model results were based entirely on the 'flat bed' formulation. Here instead, in the subset of cases for which the bed was predicted to comprise steep ripples having $\eta/\lambda \geq 0.12$, the two-layer 'rippled bed' model has been adopted, resulting in better overall agreement with the data. The equivalent results obtained using Bijker's model (Figure 3b) show a comparable level of agreement with the data.

1.5.2 Comparisons with data from Egmond Beach, The Netherlands

The results are considered from 10 tests carried out in the outer surf zone at Egmond Beach. The mean water depth was h = 1 - 2 m and the waves were superimposed perpendicularly on the longshore current. The median grain diameter of the bed material was D_{50} = 0.3 - 0.35 mm, considerably larger than at Boscombe and Maplin. Again no observations were made of the bed roughness, but the bed was predicted to comprise low ripples in most tests.

No attempt has been made to represent cross-shore transport processes associated with wave asymmetry, the waves having simply been assumed to be sinusoidal. Only transport in the longshore (i.e. mean current) direction has been considered; specifically, comparisons have been made with field estimates of the 'current-related' component (Q_s) of the suspended load transport (see Figure 4). The overall agreement for the TKE-model is encouraging, with little bias evident around the perfect agreement line, and with individual cases generally lying within a factor of ±5. In contrast, Bijker's model tends to overestimate Q_s in those cases in which the measured values of Q_s were relatively low, while it gives better agreement where values of Q_s were high.

In Figure 5 the model predictions are compared with measured profiles of mean concentration for two tests. In Test 4C (Figure 5a) the waves were relatively low (H_s/h = 0.4), making this a suitable case for comparison with the models, neither of which takes account of wave breaking effects. For the TKE model, the agreement is quite reasonable, though the concentration is over-predicted for $z/h < 0.2$ (z = height above bed) and under-predicted for $0.4 < z/h < 0.6$ due possibly to turbulence caused by the reported, occasional, wave breaking. In Bijker's model the concentration gradient is smaller, and the concentration is over-predicted at all heights. In Test 4B (Figure 5b) the waves were larger (H_s/h = 0.5) with spilling breaking reported. Here the agreement between the models and the measurements is satisfactory for $z/h \leq 0.1$, but above this the concentration is greatly under-predicted, particularly by the TKE model. This is not surprising in view of the expected effect of turbulence generated by wave breaking.

In order to explain the pattern in the results in Figure 4, the role of the relative wave height is explored further in Figure 6, where the ratio of predicted to measured, current-related, suspended transport rates is plotted against H_s/h. For the two lowest values of H_s/h the bed was predicted to comprise steep ripples (η/λ = 0.13 and 0.16), and so here the 'rippled bed' version of the TKE model was implemented. Although Q_s is under-predicted in these two cases, a

greater under-prediction would have resulted from use of the 'flat bed' TKE-model. Although rather lower ripple steepnesses were predicted for the cases corresponding to H_s/h = 0.3 - 0.4, these steepnesses may still have been too large since near-bed concentrations are over-predicted (c.f. Figure 5a for test 4C) leading to an over-prediction in Q_s. For $H_s/h > 0.5$ spilling breakers were observed, leading to an under-prediction in concentration (c.f. Figure 5b for test 4B) and, hence, to an under-prediction in Q_s. This is not surprising since the model does not include breaking-wave effects. While Bijker's model over-predicts Q_s for smaller values of H_s/h ($\leq$0.4), it provides more accurate predictions for larger values of H_s/h ($\geq$0.5). This suggests the possible advantages of scaling the empirical 'constant b' in Bijker's model on H_s/h, rather than assuming the present fixed value (b = 5).

1.5.3 Accuracy of the model predictions

An assessment of the accuracy of the model predictions may be made from the results in Figures 2 to 5. In individual cases, both models agree with the measurements of concentration and transport rate invariably within a factor of ±10, and very often within a factor of ±5. The fact that such a high degree of uncertainty exists for individual field tests is not surprising. The data considered here is sometimes not self-consistent (e.g. closely similar wave and current conditions can be associated with significant variability in measured concentrations), and knowledge about the model inputs is often poor compared with the precise definition of the conditions in laboratory work. It may be the case that factor of ±5 agreement is not unreasonable when an untuned model is applied in field conditions.

What may be a more relevant measure than the uncertainty in individual cases is the *bias* of the model results over all the tests at a particular site. This is quantified here by considering the ratios of predicted to measured concentration, and also transport rate (c.f. Figure 6), for all the field cases considered earlier. Factors of 'overall bias' have been calculated by determining the logarithms of the individual ratios in question, and then taking the anti-logarithm of the average of these values. The resulting values of the bias, with unity representing 'no bias', are shown in Table 4. For the Boscombe tests, the 'bias' in the TKE model corresponds to an over-prediction in concentration by 50% at the lower height, and an under-prediction by more than an order of magnitude at the upper height. In contrast, Bijker's model over-predicts the concentration at both heights, by factors of more than 6 and 2 times at the respective levels. For Maplin, both models perform rather better, with the TKE model under-predicting the measured concentrations by only 30% on average. For the suspended transport rates (Q_s) at Egmond, the TKE-model also performs well, with little overall bias, while Bijker's model over-predicts Q_s by a factor of 2.7 due, in part, to the use of b = 5 for Bijker's empirical constant. The bias in Q_s could be reduced significantly if the value of 'b' was linked to the relative wave height (H_s/h)

1.6 Discussion

The comparisons for the three field sites suggest that, provided research models are adapted for field use, they can be used to predict suspended concentrations and transport rates with as much accuracy as practical engineering models such as that of Bijker. This in itself is, of course, no great advance since practical models may be run far more readily than most research

models. However, the 'added value' of research models makes their use in practical situations instructive and potentially advantageous. Most importantly, research models make intra-wave predictions that allow the 'wave-related' component of the transport to be quantified. This can contribute substantially to the net transport rate, particularly for coarser sand grains confined to the oscillatory boundary layer, and can produce quite complicated, sometimes counter-intuitive, behaviour in both the cycle-mean reference concentration and also the direction of net sediment transport.

By way of illustration, consider the TKE model solution for conditions corresponding to Boscombe test B22. Here the depth-mean current was U_c = 0.295 m/s, the water depth was h = 5 m, the waves were characterised by H_s = 0.98 m, T_m = 6.74 s and U_w = 0.603 m/s, and the bed forms were predicted to comprise low ripples (η = 6 mm, λ = 97 mm). This case has been chosen since the angle of wave attack was 45°, giving rise to pronounced angular variations in the boundary layer flow and sediment transport.

The 'wave-related' component of the transport arises as follows. If the instantaneous horizontal velocity $\boldsymbol{u} = (u,v)$ and the concentration c, both at height z, are expressed as the sum of mean and periodic (or wave) contributions, as follows:

$$\boldsymbol{u} = <\boldsymbol{u}> + \boldsymbol{u}_w \qquad c = <c> + c_w,$$

where < .. > indicates a time average over an integral number of wave cycles, then the mean (mass) transport rate per width of flow is given by :

$$\rho_s <\boldsymbol{u}c> = \rho_s <\boldsymbol{u}><c> + \rho_s <\boldsymbol{u}_w c_w>$$

where ρ_s is the sediment density, and the terms on the right hand side are respectively the 'current-' and 'wave-related' components of the 'true' transport rate. The profiles of current-related and true suspended flux in the nominal current -alone direction are shown for test B22 in Figure 7a. Only the bottom 0.05 m of the flow is shown, and here a substantial difference is evident between the (smaller) current-related and (larger) true fluxes, both profiles exhibiting maximum values close to the bed.

Consider next the direction of the suspended flux. Due to the greater turbulence intensity in the 'wave-plus-current' half cycle than in the 'wave-minus-current' half cycle, the direction of the mean current veers away from that of the waves. This is shown, for the bottom 3 m of the flow, in Figure 7b in which the dots represent the tips of the velocity vectors at every third computational level. The veering angle is maximum near the bed (17°) and, although it decreases with increasing height, veering is predicted all the way up to the free-surface (where it is about 5°). The 'current-related' sediment flux follows by definition the direction of the mean current. So, as shown by the flux vectors in Figure 7c for successive computational levels through the bottom 0.06 m, the current-related flux veers away from the wave direction by about 15°. Figure 7c also shows the 'true' flux vectors, which exhibit a very different behaviour. Because peak stresses, and hence concentrations, occur near the bed in the 'wave-plus-current' half cycle, the net transport (suspended load and bed load) tends to veer into the wave direction. Above this, the direction of the net flux becomes rather variable with height and, in the present case, actually veers away from the wave direction above a height of about 0.03 m.

When the velocities in Figure 7b and the sediment fluxes in Figure 7c are integrated over the depth, the final results for the transport rate are as shown in Figure 7d. The depth-mean current (0.295 m/s) veers away from the wave direction by 5°, while the current-related, suspended load, transport (0.080 kg/m/s) veers by 14°. In contrast, the true suspended

transport rate (0.096 kg/m/s) veers *towards* the wave direction by 1°. [Note that the vector plots in Figures 7b and 7c represent results at each node in the computational grid. Since the grid is logarithmically distributed, the influence on the transport rate of those vectors with small veering angles is disproportionately large.] Also shown in Figure 7d is the net bed load transport rate. This has magnitude 0.025 kg/m/s and it also veers strongly into the wave direction. Finally, the total load transport rate, the vector sum of the bed load and true suspended load transport rates, has magnitude 0.120 kg/m/s and veers at an angle of 3° into the wave direction.

The results in Figure 7d have clear implications for grain size sorting. Coarser grains moving as bed load, or in suspension in the lower part of the oscillatory boundary layer, are predicted to veer away from the nominal current direction and into the wave direction. In contrast, finer grains travelling in suspension in the outer part of the oscillatory boundary layer may experience only a small veering effect, while still finer grains in suspension in the outer current boundary layer may veer away from the wave direction. So, if the mean current is in the longshore direction off a beach, outside the breaker zone say, coarser grains will tend to migrate onshore, while finer grains will tend to migrate offshore. This is consistent with the common observation that beach material includes little or no very fine sand.

1.7 Conclusions

The predictions of a research (TKE) model and the practical sand transport model of Bijker (1971) have been compared with data obtained in combined wave-current conditions at three field sites. The results demonstrate that, provided research models are adapted for field application, they may be used to make practical sand transport computations with as much accuracy as practical engineering formulations. Both models have been run here using values of the bed roughness (k_s) that have been estimated on the basis of a prediction scheme for the dimensions of sand ripples. The comparisons between suspended sand concentrations and transport rates show that a considerable amount of uncertainty (factor ±5 or more) arises when the individual predictions of either model are compared with the measurements. However, the overall bias in each set of comparisons is smaller than this, with overall agreement being within a factor of ±2 in most cases. Compared with the previously published predictions of DV2000, the present results have been improved in the case of the TKE model by the inclusion of a 'rippled bed' sub-model for cases in which vortex shedding is likely to have occurred above (steep) sand ripples on the bed. In the case of Bijker's (1971) model, the level of agreement with the measurements could probably be improved by expressing the empirical 'constant *b*' as a function of the relative wave height. However the greatest single obstacle to making sand transport predictions remains the accurate estimation of the seabed ripple dimensions and, hence, the bed roughness (k_s).

Although the satisfactory use of research models to make practical computations may be viewed as an important justification for their development, the primary role of research models lies in the improved understanding of detailed sediment transport processes that they provide. This has been illustrated here with reference to the mechanism of grain size sorting resulting from the oblique incidence of waves on a current. The ability of research models to represent intra-wave processes, and thereby illuminate subtle and sometimes counter-intuitive mechanisms, remains their true benefit.

1.8 Figures

List of figures

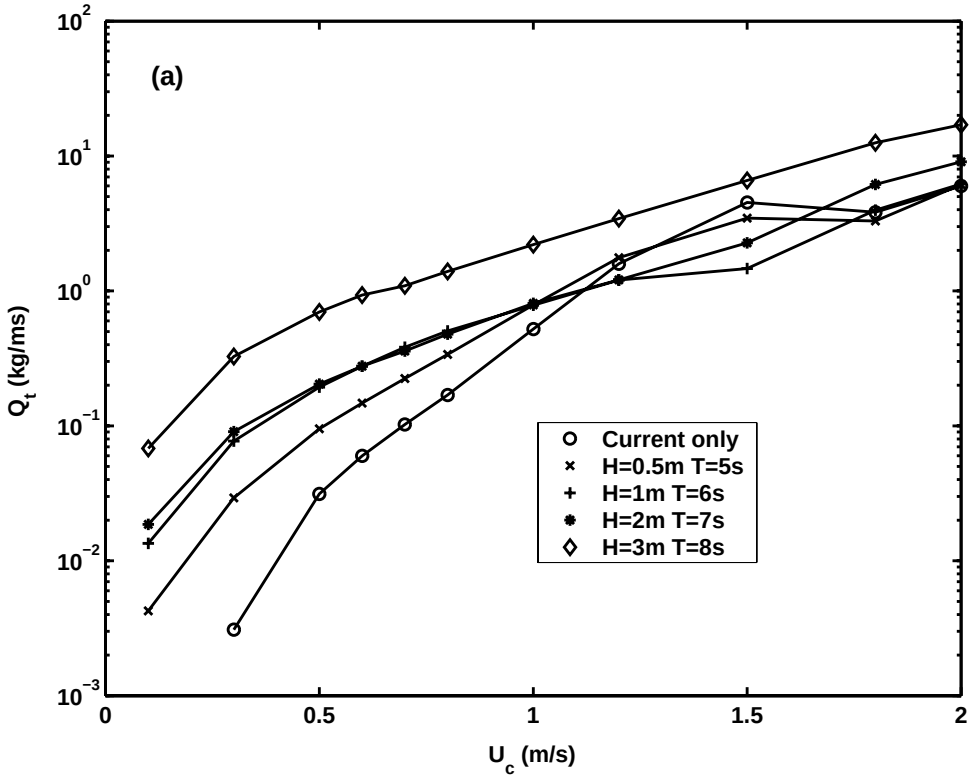

Figure 1a

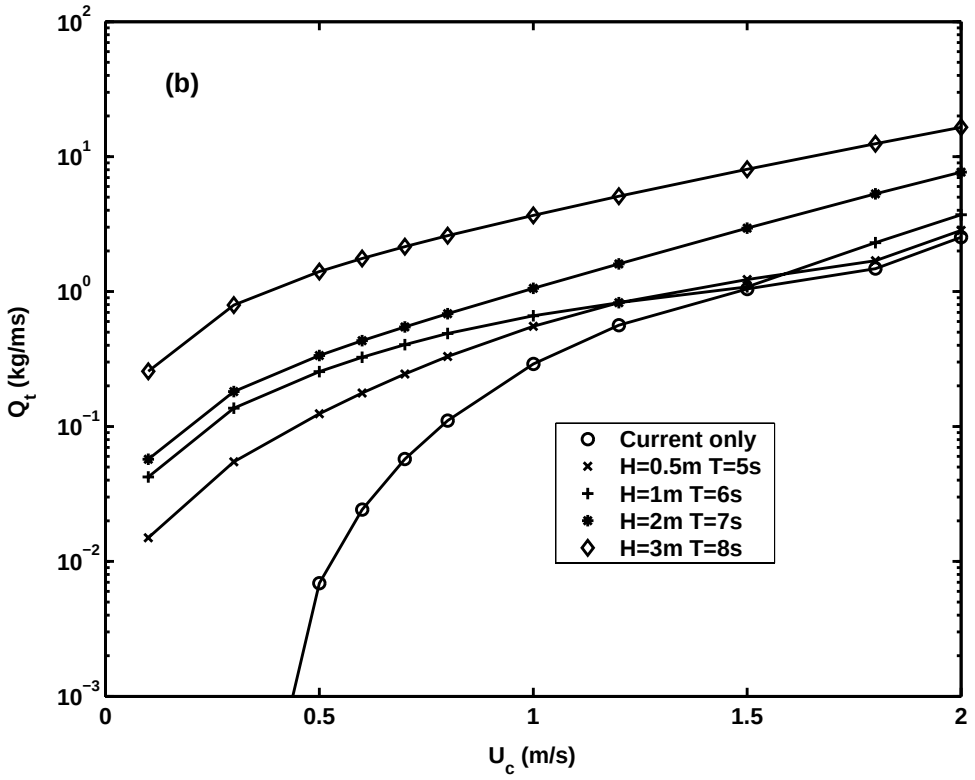

Figure 1b

Fig. 1. Comparison between total sediment transport rates (Q_t) given by (a) the TKE-model and (b) Bijker's model. The respective lines with symbols denote the current alone and the current combined with the four waves. The bed roughness (k_s) and suspended sand size (D_s) have been predicted using the methods discussed.

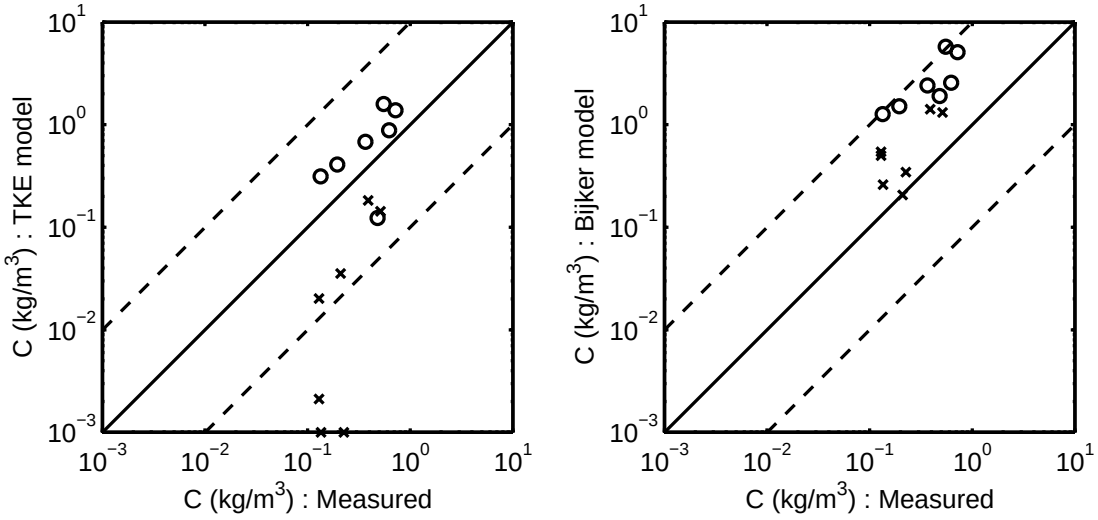

Fig. 2. Boscombe Pier tests: (a) comparison between measured and predicted (TKE model) suspended sediment concentrations at heights 0.1 m (o) and 0.5 m (x); (b) equivalent comparison between the measured concentrations and Bijker's model.

Perfect agreement is indicated by the full 45° line, and factor ±10 agreement by the dashed lines.

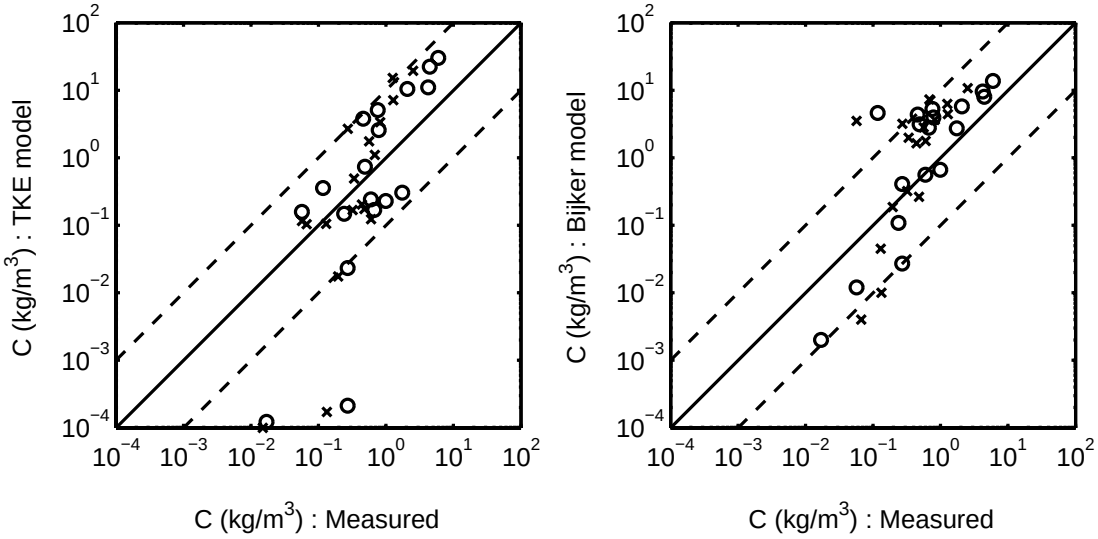

Fig. 3. Maplin Sands tests: the comparisons in (a) and (b) are as in Figure 2 but with concentrations measured at heights 0.05 m (o) and 0.1 m (x).

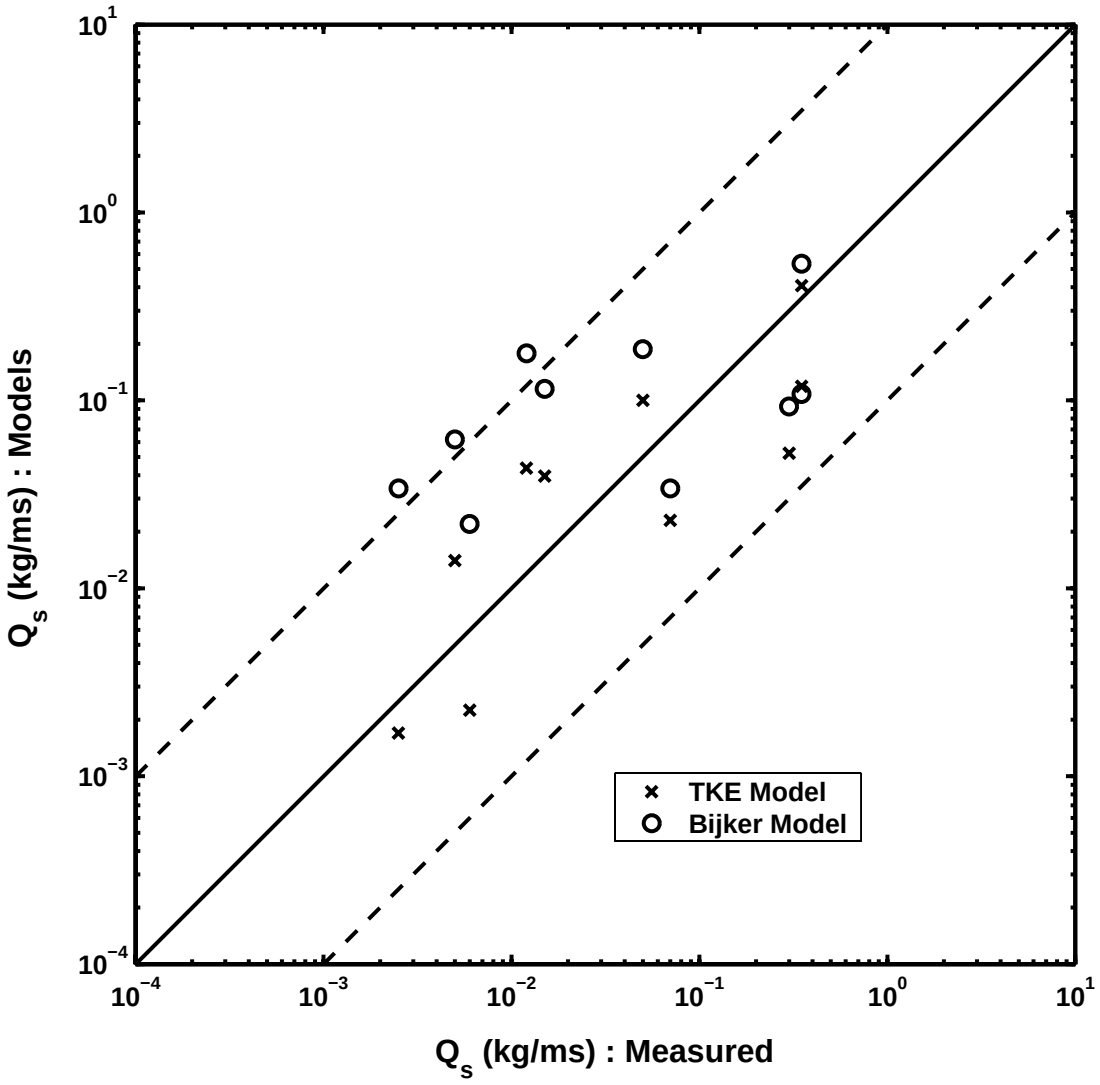

Fig. 4. Egmond Beach tests: comparison between predicted (TKE and Bijker models) and measured suspended sediment transport rates (Q_s). The field estimates of Q_s are for the current-related component of the transport only.

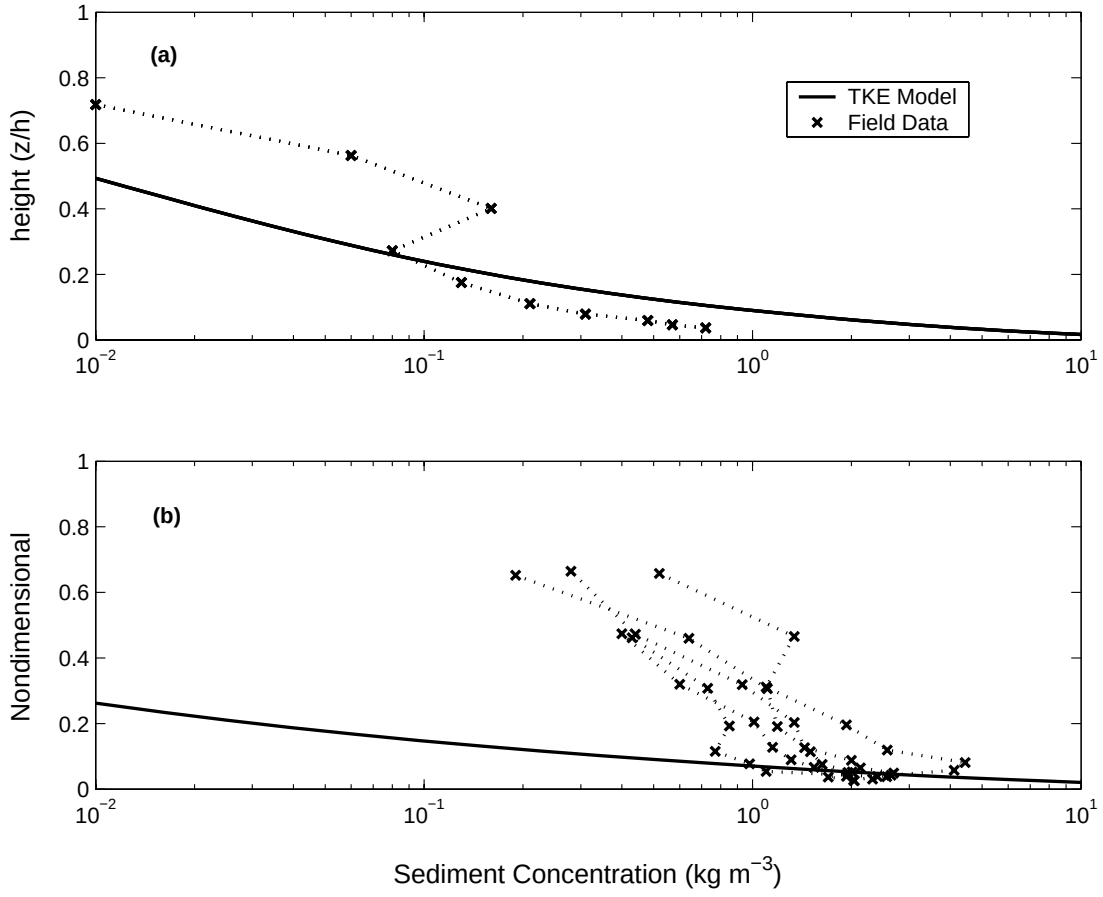

Fig. 5. Egmond Beach tests: comparison between predicted (TKE and Bijker models) and measured mean concentration profiles for (a) test 4C and (b) test 4B.

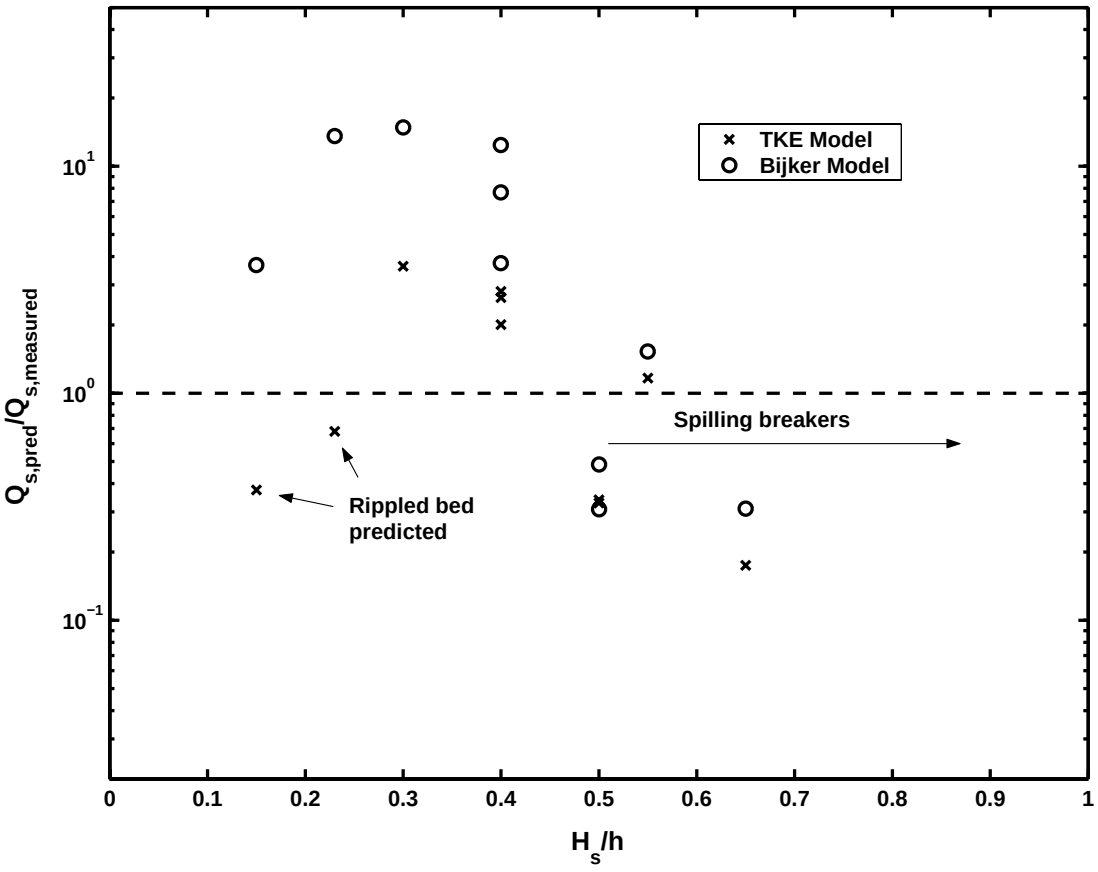

Fig. 6. Egmond Beach tests: ratios of predicted to measured suspended sediment transport rate Q_s ('current-related' component) as a function of the relative wave height H_s/h (H_s = significant wave height, h = water depth).

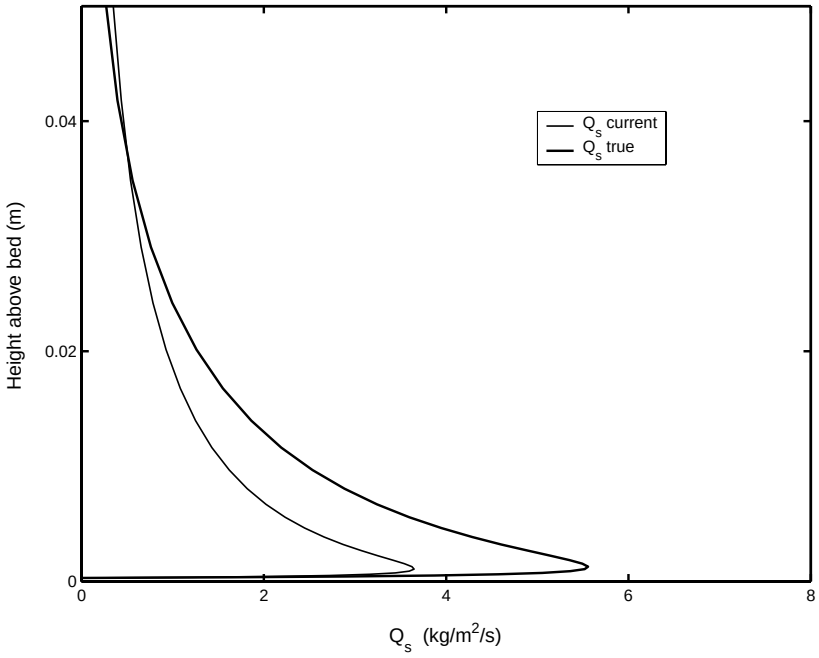

Figure 7.a: Vertical profiles of suspended sediment flux in the bottom 0.05 m (full line, 'true' flux; dashed line, 'current-related' component);

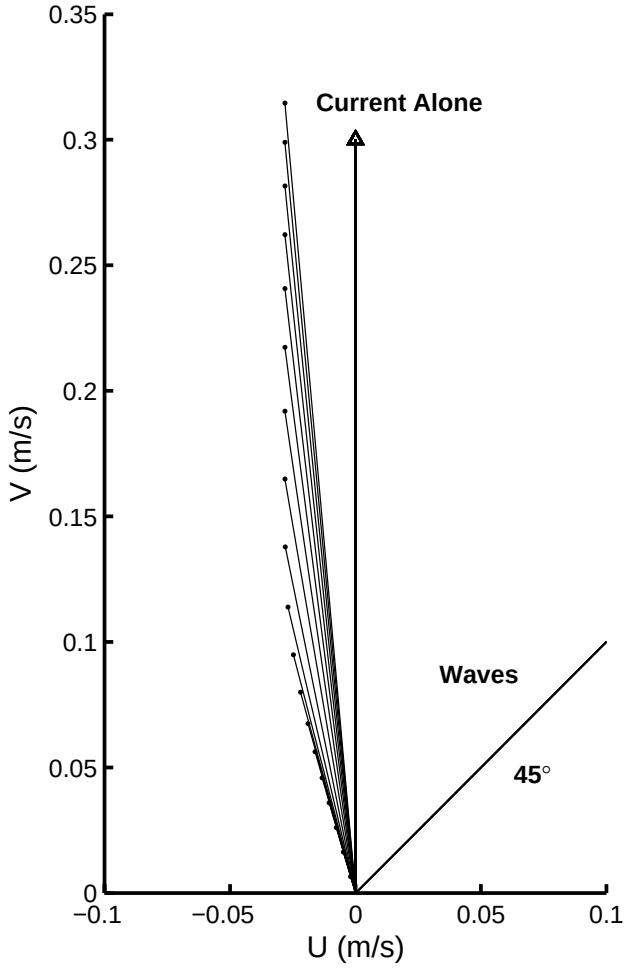

Figure 7.b: Veering of the mean velocity vectors in the bottom 3 m

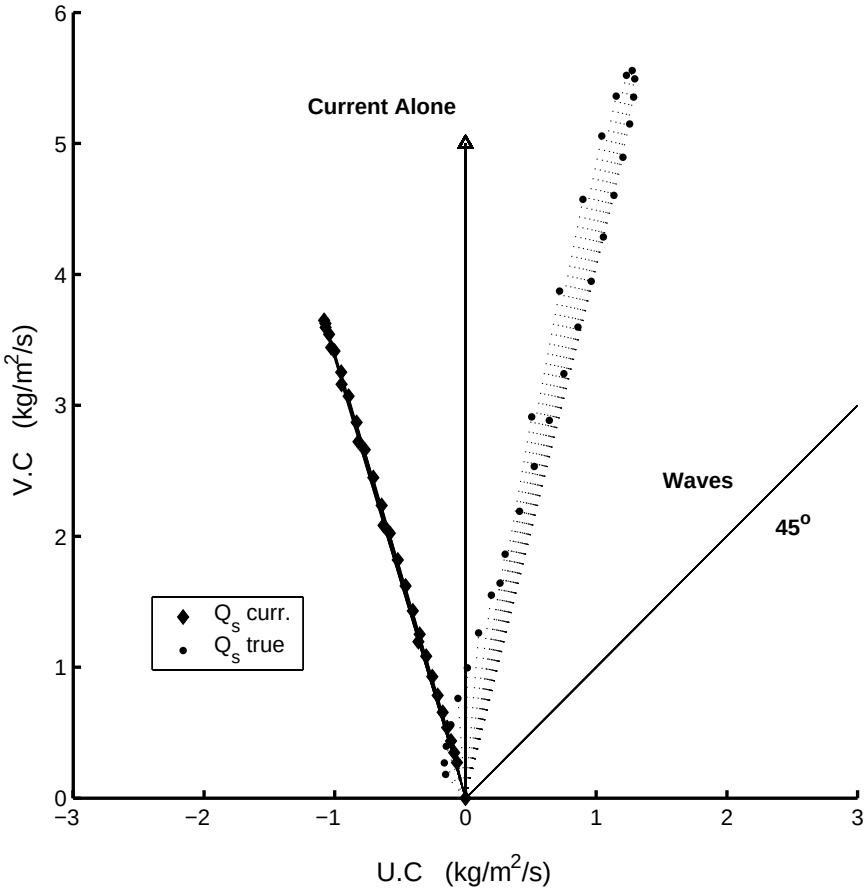

Figure 7.c: Veering of the 'true' and 'current-related' suspended sediment flux vectors in the bottom 0.06 m

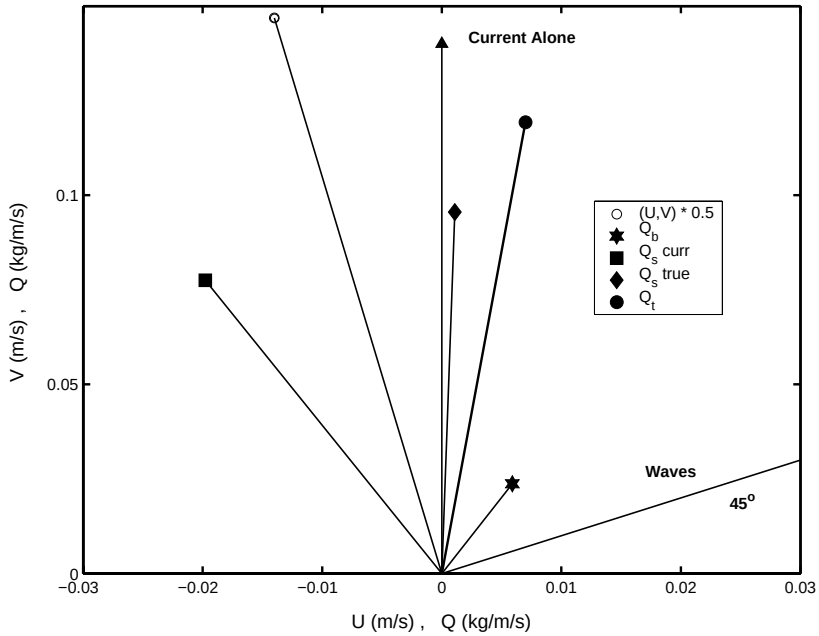

Figure 7.d : Magnitude and direction of the depth-averaged velocity, and also of the total net transport rate (Q_t), and of its components (Q_b, Q_s). The scales on the horizontal and vertical axes are unequal for clarity of illustration.

Fig. 7. TKE model predictions for Boscombe Pier test B22

1.9 References

Bijker, E.W., 1971. Longshore transport computations. Journal of Waterways, Harbours and Coastal Engineering Division, American Society of Civil Engineers, 97 (WW4), 687-701.

Bijker, E.W., 1992. Mechanics of sediment transport by the combination of waves and current. In Design and Reliability of Coastal Structures, 23rd International Conference on Coastal Engineering, American Society of Civil Engineers, pp.147-173.

Davies, A.G., Li, Z., 1997. Modelling sediment transport beneath regular symmetrical and asymmetrical waves above a plane bed. Continental Shelf Research 17 (5), 555-582.

Davies, A.G., Villaret, C., 1999. Eulerian drift induced by progressive waves above rippled and very rough beds. Journal of Geophysical Research 104 (C1), 1465-1488.

Davies, A.G., Ribberink, J.S., Temperville, A., Zyserman, J.A., 1997. Comparisons between sediment transport models and observations made in wave and current flows above plane beds. Coastal Engineering 31, 163-198.

Davies, A.G., Villaret, C., 2000. Sand transport by waves and currents: Predictions of research and engineering models. Proceedings of the 27th International Conference on Coastal Engineering, American Society of Civil Engineers, Sydney, 2481-2494.

Engelund, F., Fredsøe, J., 1976. A sediment transport model for straight alluvial channels. Nordic Hydrology 7, 293-306.

Fredsøe, J., Deigaard, R., 1992. Mechanics of coastal sediment transport. World Scientific, Singapore, 369pp.

Hagatun, K., Eidsvik, K.J., 1986. Oscillating turbulent boundary layer with suspended sediments. Journal of Geophysical Research 91 (C11), 13045-13055.

Kroon, A., 1994. Sediment transport and morphodynamics of the beach and nearshore zone near Egmond, The Netherlands. PhD Thesis, University of Utrecht.

Li, Z., Davies, A.G., 1996. Towards predicting sediment transport in combined wave-current flow. Journal of Waterway, Port, Coastal and Ocean Engineering, American Society of Civil Engineers 122 (4), 157-164.

Li, Z., Davies, A.G., 1997. Effects of grain size gradation and reference concentration on sediment transport beneath large waves. Proceedings of Coastal Dynamics '97, American Society of Civil Engineers, pp. 245-254.

Li, Z., Davies, A.G., 2001. Turbulence closure modelling of sediment transport beneath large waves. Continental Shelf Research 21, 243-262.

Nielsen, P., 1986. Suspended sediment concentrations under waves. Coastal Engineering 10, 23-31.

Soulsby, R.L., 1998. Dynamics of marine sands. Thomas Telford, England.

Tanaka, H., Dang, V.T., 1996. Geometry of sand ripples due to combined wave-current flows. Journal of Waterway, Port, Coastal and Ocean Engineering, American Society of Civil Engineers, 122 (6), 298-300.

Van Rijn, L.C., 1973. Principles of sediment transport in rivers, estuaries and coastal seas. Aqua Publications, Amsterdam.

Van Rijn, L.C., Davies, A.G., Van de Graaff, J., Ribberink, J.S., 2001. SEDMOC: Sediment transport modelling in marine coastal environments. Aqua Publications, Amsterdam.

Whitehouse, R.J.S., Thorn, M.F.C., Houghton, P.J., 1996. Sediment transport measurements at Maplin Sands, Outer Thames Estuary. Data Report. HR Wallingford, Report TR15.

Whitehouse, R.J.S., Owen, M.W., Stevenson, E.C., 1997. Sediment transport measurements at Boscombe Pier, Poole Bay. HR Wallingford, Report TR27.

Wiberg, P.L., Harris, C.K., 1994. Ripple geometry in wave-dominated environments. Journal of Geophysical Research 99 (C1), 775-789.

Wolf, F.C.J., 1997. Hydrodynamics, sediment transport and daily morphological development of a bar-beach system, Egmond, The Netherlands. PhD Thesis, University of Utrecht.

2. Sediment transport modelling for coastal morphodynamics

Abstract: The accurate prediction of sand transport rates in the coastal zone depends not only upon the choice of sediment transport model but also, rather critically, upon the formulation used to predict the bed roughness (k_s). Sand transport rates are modelled here using both a One-equation, turbulence-closure, TKE-model and also Bijker's sand transport model. Following some remarks about the nature and importance of sand ripples, results corresponding to a wide range of combined wave and current conditions are obtained based upon both prescribed and predicted values for k_s. The substantial difference between the two sets of results highlights the importance of predicting k_s as accurately as possible in situations in which the bed roughness is not known. An example involving waves incident on a plane sloping beach is used to illustrate the variations in ripple dimensions, and hence, k_s, likely to be found in a typical coastal domain. Here Bijker's model has been implemented within the TELEMAC Modelling System to predict the longshore sand transport rate. It is shown that the inclusion of *local* variations in k_s within the study area approximately halves the longshore transport rate compared with results based on the use of a constant, prescribed values of k_s throughout the domain. The possible consequences of bed roughness variations are discussed briefly in the context of morphological modelling.

2.1 Introduction

The accurate quantification of local sand transport rates in the marine coastal environment is a prerequisite for the prediction of seabed changes and coastline evolution. In an intercomparison with laboratory data in the EU MASTII G8-M Project (1992-5), it was found that four different research models predicted net sediment transport rates beneath asymmetrical waves, and also in collinearly combined wave and current flows, to well within a factor of 2 of the measured values (Davies et al., 1997). In addition, cycle-mean sediment concentration profiles were predicted to good accuracy. However, the range of conditions investigated was quite narrow, involving sheet flow (i.e. plane beds) only. A more recent series of model intercomparisons, and model comparisons with field data, carried out over a wider range of conditions during the EU MASTIII SEDMOC Project (1998-2001), suggested far less convincing agreement between the models and the data, and suggested that large gaps still remain in our knowledge of sand transport processes (Davies et al., 2002).

Initially, in the SEDMOC study, seven 'research' models were intercompared over a wide range of wave and current conditions, corresponding to both plane and rippled sand beds. These models included both one-dimensional vertical (1DV) formulations, varying in complexity from eddy viscosity and mixing length models to a full two-phase flow formulation, and also 2DV formulations capable of representing vortex shedding above sand ripples. The model results showed greatest convergence for cases involving plane beds, with predicted sand transport rates agreeing to well within an order of magnitude, and greatest divergence for cases involving rippled beds. A similar intercomparison involving (mainly) 'practical' sand transport models, carried out over wide wave and current parameter ranges,

also showed greatest variability in cases involving rippled beds. Finally, (mainly) practical models were compared with field data obtained at five contrasting field sites. The results showed that suspended sand concentrations in the bottom metre of the flow were predicted within a factor of 2 of the measured values in 13% to 48% of the cases considered, and within a factor of 10 in 70% to 83% of the cases, depending upon the model used. Estimates of the measured longshore component of suspended sand transport yielded agreement to within a factor of 2 in 22% to 66% of cases, and within a factor of 10 in 77% to 100% of cases, again depending upon the model used.

The results of the SEDMOC study suggest that, at the present stage of research, considerable uncertainty should be expected if untuned models are used to make *absolute* predictions for field conditions, and that the availability of some measurements on site is still a necessary requirement for high-accuracy sand transport predictions. However, for morphological modellers, the results were considered to be more encouraging, since many of the models exhibited agreement in their *relative* behaviour over wide ranges of wave and current conditions, which is a prerequisite to obtaining correct morphodynamic predictions.

In the present paper, the importance of the bed roughness (k_s)is highlighted in relation to sediment transport computations. Following a discussion of the general role of sand ripples, a procedure is outlined for the prediction of the dimensions of ripples and, hence, of the bed roughness k_s, in combined wave-current flow. Results are then presented that illustrate the sensitivity of sediment transport rate to the choice of bed roughness over a range of wave-current conditions. Finally, an illustrative example is presented involving waves that are incident, both normally and obliquely, on a beach. The variability in the predicted bed roughness k_s as the waves shoal and then break is illustrated. In the case of oblique wave incidence, the effect on the longshore sand transport rate of the use of a locally predicted bed roughness, as opposed to a constant (specified) bed roughness over the entire study area is demonstrated. The wider implications of these results for morphological modelling are discussed briefly.

2.2 Sand ripples and bed roughness

One of the central considerations involved in obtaining reliable sediment transport rate predictions is the accurate specification of the bed roughness. In practice, depending upon the local wave-current conditions and seabed composition, potentially significant variations in the roughness may occur within a coastal area. For example, in deeper water where the wave conditions are relatively inactive, steep sand ripples may occur while, in shallower water where the waves become nonlinear and ultimately break, low ripples or plane bed conditions are likely to be found. If a morphological model does not account for the consequent local variations in bed roughness, significant errors may arise in the pattern of transport rates throughout the study area. Both rippled and plane beds have considerable practical importance, and both require appropriate modelling approaches.

Since large areas of the seabed comprise relatively steep sand ripples, it is unfortunate that, as noted above, our present ability to model transport above rippled beds is less certain than above plane beds (‘sheet flow’ conditions). This is true of both practical formulations, and also detailed research models (see Davies et al., 2002). In practice, some of this uncertainty arises from the choice of the bed roughness. However, at least in the case of

research models, further uncertainty can arise from the way in which reference concentration formulae (or pick up functions) are implemented by modellers above rippled beds. In the SEDMOC study, this latter uncertainty led to variations in the predicted transport rate of between 1 and 2 orders of magnitude (Davies et al., 2002).

There is an essential difference between the sediment transport processes that occur above rippled and plane sand beds (see, for example, Nielsen (1992), Fredsøe and Deigaard (1992), Van Rijn et al. (2001)). It is important therefore to define the boundary delineating these regimes. Steep ripples are formed by relatively low waves in relatively deep water (i.e. typical offshore conditions). Such ripples tend to be long crested (two-dimensional), and have steepness (η/λ) greater than about 0.15, where η and λ are the ripple height and length, respectively. The 'roughness' (k_s) of a rippled bed is normally equivalent to about 3-4 ripple heights ($k_s = 3\eta$- 4η). Beneath steeper waves in shoaling water, the ripples start t to become shorter crested (transitional 2D-3D profiles); here their steepness decreases, causing k_s to decrease. Finally, beneath very steep and breaking waves, the ripples may be 'washed out' completely, the bed becomes plane ('sheet flow' regime), and the bed roughness k_s decreases still further (scaling on the sand grain diameter). This sequence is summarised in Table 1 below in terms of the non-dimensional 'relative roughness' A_0/k_s, where A_0 is the near-bed orbital excursion amplitude. For cases of practical interest in the sea it is possible to associate with the respective ranges of A_0/k_s, equivalent approximate ranges of wave Reynolds number RE ($=A_0^2\omega/\nu$), where ω = wave angular frequency and ν = kinematic viscosity, as indicated above. The type of oscillatory boundary layer flow expected in different ranges of A_0/k_s and RE has been reviewed by Davies and Villaret (1997).

Table 1. Bed form characteristics in the coastal zone

Bed form characteristics	2D Steep Ripples	2D and 3D Low Ripples	Washed-out Ripples	Plane Bed
Ripple steepness η/λ	$\eta/\lambda \geq 0.15$	$0.05 < \eta/\lambda \leq 0.15$	$\eta/\lambda < 0.05$	$\eta/\lambda = 0$
Relative roughness A_0/k_s	O(1)	O(1-10)	O(10-100)	O(100-1000)
Reynolds number RE	$O(10^3\text{-}10^4)$	$O(10^4\text{-}10^5)$	$O(10^5)$	$O(10^6\text{-}10^7)$

Above plane beds in oscillatory flow, momentum transfer occurs primarily by turbulent diffusion and may, together with the associated sediment transport, be modelled using conventional turbulence-closure, numerical, schemes. Such schemes may include detailed treatment of the very near-bed, sheet flow layer (see, for example, Malarkey et al., 2002). In contrast, above rippled beds, momentum transfer and the associated sediment dynamics are dominated in the near-bed layer by coherent motions, specifically by the process of vortex formation above ripple lee slopes, and the shedding of these vortices at flow reversal. Above steep, long-crested ripples, with height to wavelength ratio greater than about 0.12, this well-organised, 'convective' process of vortex formation and shedding is highly effective in entraining sand into suspension. The rough turbulent oscillatory boundary layer above rippled beds is considerably thicker than that above plane beds, the boundary layer consisting of a lower layer dominated by the vortex shedding process and an upper layer in which the coherent motions break down and are replaced by random turbulence. This leads to the entrainment of sediment into suspension to considerably greater heights than above plane beds. In combined wave and current flow above ripples, the outer part of the boundary layer structure referred to above merges with the turbulent 'current' boundary layer, into which

sediment can be entrained into suspension to still greater heights.

Several modelling studies of two-dimensional horizontal-vertical (2DHV) oscillatory flow above rippled beds have sought to represent the formation and shedding of vortices, and the subsequent trajectories of the (decaying) vortices (Longuet-Higgins, 1981; Blondeaux and Vittori, 1991; Hansen et al., 1994; Malarkey and Davies, 2002). Sediment in suspension above ripples has been modelled by Hansen et al. (1994), Block et al. (1994), and Andersen and Fredsøe (1999). Although 2DHV-models have achieved reasonable success in representing the main features of vortex dynamics and the associated sediment transport above rippled beds, such models are unduly complex from an engineering point of view. For the most part, existing engineering models attempt to represent ripples by simply enhancing the bed roughness k_s used in standard, one-dimensional vertical (1DV) 'flat bed' formulations. This approach has some merit for low ripples (Davies and Villaret, 2000), but has severe conceptual limitations for steep ripples. Appropriate time-mean formulations for the eddy viscosity and sediment diffusivity above rippled beds, for use in a horizontally-averaged 1DV framework, have been proposed by Nielsen (1992) and Sleath (1991), and by Nielsen (1992), respectively. They presented empirical evidence to show that, in contrast to the plane bed case, a height-independent mean viscosity is appropriate in the near-bed vortex layer above ripples. Subsequently, it was shown by Davies and Villaret (1997, 1999) that time-variation in the eddy viscosity is more pronounced above ripples than above plane beds, with peaks in viscosity occurring near times of flow reversal. Davies and Thorne (2002) have presented recently a relatively simple, 1DV modelling approach that includes a time-varying eddy viscosity of this type. This model represents both intra-wave flow and sediment transport processes, and also the near-bed wave-generated residual currents above the ripples.

ESTIMATION OF BED ROUGHNESS (k_s)

Davies and Villaret (2000) suggested the following procedure for the calculation of the bed roughness k_s in combined wave-current flow, based on the formulations of Wiberg and Harris (1994) and Tanaka and Dang (1996). Since the strength of any mean current present at the edge of the (thin) oscillatory boundary layer is relatively small (Andersen and Fredsøe, 1999), the waves may be taken as the starting point in the estimation of the bed roughness. The formulation of Wiberg and Harris (1994) for waves alone has thus been used initially to calculate the wavelength (λ) and steepness (η/λ) of the seabed ripples. A non-iterative procedure for the calculation of η and λ using Wiberg and Harris' formulation has been presented recently by Malarkey and Davies (2003).

To allow for the superimposition of a current on the waves, the orbital diameter d_0 ($=2A_0$) is next replaced by αd_0 using the parameter α proposed by Tanaka and Dang (1996) for collinear wave-current flows. Further, in order to allow for the superimposition of waves on a current at any angle of attack φ, the following generalised definition of α has been adopted:

$$\alpha = 1 + 0.81\left[\tanh(0.3S_*^{2/3})\right]^{2.5}\left(U_c\cos(\varphi)/U_w\right)^{1.9}$$

where S_* = immersed specific weight of sand. This formula differs from that of Tanaka and Dang (1996) by the inclusion of the term $\cos(\varphi)$, which has the effect of combining the waves with the resolved component of the current in the wave direction. No distinction has been made between following and opposing currents. Finally, in order to ensure that the ripples in general angular cases are not unrealistically steep when, for example, a strong current is combined perpendicularly with low waves, a 'maximum steepness' criterion

$(\eta/\lambda)_{max} = f(\theta'_{max})$ has been imposed (θ'_{max}= peak, skin friction, Shields parameter). The function $f(\theta'_{max})$ used here is similar to Nielsen's (1992) expression. Finally, the predicted values of η and λ have been used to define the bed roughness (k_s). In the TKE-model discussed shortly, the following rule has been adopted

$$k_s = 25\eta(\eta/\lambda) + 5\theta' D$$

where the terms on the right hand side represent respectively the ripple roughness (c.f Swart, 1976) and the mobile bed roughness (c.f. Wilson, 1989). In Bijker's (1971) model, also discussed below, the specified rule $k_s = \max(\eta, D_{90})$ is used.

2.3 Use of prescribed versus predicted ks in the calculation of sand transort rates

To illustrate the sensitivity of sediment transport rate predictions to the choice of bed roughness k_s, results are presented here based upon both prescribed and predicted values of k_s. Two models are considered: i) the 'TKE model' of Davies and Li (1997) and ii) Bijker's (1971, see also 1992) sand transport model.

The 'TKE model' is a local, one-dimensional (vertical) numerical formulation, based on a One-Equation, turbulent kinetic energy (TKE) closure. The model, which predicts both intra-wave and cycle-mean sediment concentrations and fluxes, has been (i) adapted to allow it to be run in 'flat bed' cases ($\eta/\lambda \le 0.12$) with any prescribed or predicted bed roughness k_s, and (ii) extended to allow it to be run in 'rippled bed' cases ($\eta/\lambda \ge 0.12$). Further details about the implementation of this model have been given by Davies and Villaret (2000, 2002).

Bijker's (1971) model is long established, and used widely by practising engineers due to its ready implementation and also the fact that its predictions are broadly similar to those of more complicated, practical models. It also has the appeal of being based on classical sediment transport concepts for the bed load and suspended load, rather than relying on empirical curve fitting to transport data. [In the present implementations, Bijker's coefficient b has been taken as b=5.] Bijker's model takes account of the presence of ripples on the bed simply through the prescription of k_s. However, the determination of ripple height (η) is left to the user. As noted by Davies and Villaret (2000), for combined waves and currents the formulation adopted by Bijker for the mean shear stress is highly non-linear, particularly for waves superimposed on weak currents.

The comparisons in this section involve several currents alone, and four waves combined with these currents at an angle of attack of $\pi/2$ in water of depth 5m, temperature 15° and salinity $0‰$. The parameter settings are those used originally by Van Rijn (1993, Appendix A). As shown in Table 2, the depth-mean velocity (U_c) varies in the range 0.1-2m/s. The four waves, referred to as 'Waves 1 to 4', are defined by their significant heights (H_s) and peak periods (T_p). Following the approach of Van Rijn (1993) the waves have been treated as purely sinusoidal, and near-bed wave velocity amplitudes (U_w) have been calculated using linear wave theory as 0.255, 0.568, 1.207 and 1.879 m s^{-1}, respectively. The seabed sediment comprises sand having D_{50} = 0.25mm and D_{90} = 0.5mm. The bed roughness has been *prescribed* by Van Rijn (1993) as representative of field conditions, all of the prescribed

values of k_s in Table 1 being considerably larger than the granular roughness $k_s = 2.5D_{50} = 0.625$mm. For the current alone, and the current in combination with the two smaller waves, the roughness varies from $k_s = 0.1$ m ('rippled bed') to 0.02 m ('flat bed'). For the current combined with the two larger waves, the (minimum) flat bed roughness of 0.02 m is imposed throughout. In the flat bed cases, the sand size in suspension (D_s) is taken as the median size of the bed material ($D_s = D_{50}$); for the rougher beds in less active wave-current conditions, $D_s < D_{50}$ as specified in Table 2. The settling velocity (w_s) corresponding to D_s has been calculated using the formula of Van Rijn (1993).

Current Alone					
Hs=0 m					
Waves 1&2			Waves 3&4		
Hs=0.5 m	Tp=5 s		Hs=2.0 m	Tp= 7 s	
Hs=1.0 m	Tp= 6 s		Hs=3.0 m	Tp= 8 s	
Depth-mean current vel.	Bed roughness	Suspended sand size	Depth-mean current vel.	Bed roughness	Suspended sand size
U_c (m/s)	k_s (m)	D_s (mm)	U_c (m/s)	k_s (m)	D_s (mm)
0.1	0.1	0.17	0.1	0.02 (flat)	0.25
0.3	0.1	0.17	0.3	0.02 (flat)	0.25
0.5	0.1	0.17	0.5	0.02 (flat)	0.25
0.6	0.1	0.18	0.6	0.02 (flat)	0.25
0.7	0.1	0.19	0.7	0.02 (flat)	0.25
0.8	0.1	0.2	0.8	0.02 (flat)	0.25
1.0	0.1	0.21	1.0	0.02 (flat)	0.25
1.2	0.08	0.22	1.2	0.02 (flat)	0.25
1.5	0.06	0.23	1.5	0.02 (flat)	0.25
1.8	0.03	0.24	1.8	0.02 (flat)	0.25
2.0	0.02 (flat)	0.25	2.0	0.02 (flat)	0.25

Table 2. Parameter settings (c.f. Van Rijn, 1993) for runs with prescribed k_s and D_s

In Figure 1, the TKE model results based on the prescribed k_s values are presented. The five full lines show the total transport rates (Q_t) predicted by the TKE model for the current alone and, successively, for the current in combination with the four waves. The effect of waves on the transport rate is substantial, particularly for waves combined with the smaller currents. Here the predicted effect of wave stirring is to increase the transport rate by two (or more) orders of magnitude. The equivalent set of dashed curves shown in this figure represents the transport rates resulting from the use of a granular roughness, given here by $k_s = 2.5D_{50}$. There is up to an order of magnitude difference between the results obtained by assuming a rippled-bed rather than a granular roughness.

In Figure 2 the effect on the TKE-model transport predictions in Figure 1 of using predicted rather than prescribed values of the bed roughness k_s is illustrated. As part of each

calculation, the model determined the value of k_s. The resulting k_s-values in Table 3 correspond to steeply rippled beds for relatively inactive wave and current conditions, through to almost-plane beds for more active conditions, in qualitative agreement with the trends in Table 2. However, due to the variations between the two sets of k_s-values (in Tables 2 and 3), the results for transport rate in Figure 2 exhibit a complex pattern, with rippled beds tending to enhance transport and plane beds tending to inhibit transport, as revealed by the overlapping of the transport curves. This is in contrast to the non -overlapping transport curves in Figure 1 based on the prescribed k_s values. In connection with Figure 2, it should be added that the TKE-model also determined within each run the median diameter (D_s), and hence settling velocity, of the suspended sediment. The procedure used to obtain the D_s values listed in Table 3 has been explained by Davies and Villaret (2000, 2002).

In Figure 3 equivalent transport results are presented based on Bijker's model. Here the same values of the predicted height (η) have been used as for the TKE-model (Table 3), and ks has then been determined from the rule $k_s = \max(\eta, D_{90})$. For consistency with the Bikjer formulation, the settling velocity has been based simply on the median diameter (D_{50}) of the bed material. As noted earlier, in Bijker's model the superimposition of even small waves on a current produces greatly enhanced bed shear stresses and, hence, transport rates. This is reflected in the quite large differences between the transport predictions of the TKE and Bijker models, particularly for small values of the current (U_c) combined with the respective waves. A more regular pattern of transport curves is produced by the Bijker model than by the TKE-model, with less pronounced overlapping occurring on account of the variations in k_s. [Results equivalent to those in Figure 1 have been presented for the Bijker model by Davies and Villaret (2000).]

The results in Figures 1 to 3 provide an illustration of the variation between different modelling approaches, and of the substantial effect on the results of the choice of bed roughness (k_s).

Current +Wave 1 H_s=0.5 m T_p=5 s			Currents + Wave 3 H_s=2.0 m T_p= 7 s		
Depth-mean current vel. U_c (m/s)	Bed roughness k_s (m)	Suspended sand size D_s (mm)	Depth-mean current vel. U_c (m/s)	Bed roughness k_s (m)	Suspended sand size D_s (mm)
0.1	0.182	0.108	0.1	0.0024	0.224
0.3	0.179	0.113	0.3	0.0024	0.224
0.5	0.163	0.126	0.5	0.0024	0.225
0.6	0.159	0.135	0.6	0.0024	0.225
0.7	0.147	0.143	0.7	0.0024	0.226
0.8	0.132	0.152	0.8	0.0025	0.226
1.0	0.0901	0.169	1.0	0.0026	0.228
1.2	0.0433	0.184	1.2	0.0027	0.230
1.5	0.0059	0.202	1.5	0.0030	0.233
1.8	0.0017	0.216	1.8	0.0033	0.236
2.0	0.0019	0.223	2.0	0.0035	0.238

Table 3. TKE model input parameters, including predicted k_s and D_s, for the currents combined with Waves 1 & 3

2.4 Example: Waves incident on a beach

The importance of the bed roughness, and its spatial variation, for morphodynamic computations is discussed, finally, with reference to waves incident on a uniform, plane sloping beach. The TELEMAC Modelling System (v5p2) has been used here to represent waves incident on a 1km length of beach. The model domain extends to a distance of 200 m offshore where the depth (at y = 200 m) is 10 m. The depth then decreases linearly to zero at the shoreline (y = 0 m).

At the outer boundary (y = 200 m), the waves (simulated using the module TOMAWAC) have height 1 m, peak frequency 8 s, and direction to the shoreline of either 0º (normal incidence) or 45º (oblique incidence). Wave dissipation occurs as a result of both breaking and bottom friction. There is zero wind stress. The converged model solution simulates the evolution of the wave height, frequency and direction as the waves propagate towards the beach. Figure 4a shows the cross-shore variation in wave height, for both the 0º and 45º cases, at the centre of the model domain (x = 500 m). In the case of normal incidence the wave height increases steadily towards the break point at about y = 160 m, beyond which it decreases rapidly towards the shoreline. In contrast, in the case of oblique incidence, the effect of changing wave direction results in rather little variation in wave height until the

waves break at about y = 165 m. Also shown in Figure 4a is the variation in the predicted mean water level resulting from set-up and set-down. The set-up at the shoreline is quite small, amounting to 0.08 m and 0.07 m in the cases of normal and oblique incidence, respectively. The choice of lateral boundary conditions ensured that the wave conditions in both simulations were very nearly uniform in the longshore direction.

In the case of oblique (45º) wave incidence, the radiation stresses give rise to a longshore current (simulated here with the module TELEMAC2D). The converged, time-mean velocity profile, which is also very nearly uniform in the longshore direction, is shown in Figure 4b. The maximum value of longshore velocity (2.4 m s^{-1}) occurs within the breaker zone (at y = 175 m) in water of depth 1.25 m. Lateral diffusion results in the longshore current being present well beyond the breaker point.

The physical picture represented by the waves and currents shown in Figures 4a and 4b, respectively, has next been used to predict sediment transport rates. For this purpose, the model of Bijker (1971) has been used. This is one of the options available in the module SISYPHE. For simplicity, a single sediment size has been assumed here having $D_{50} = D_{90}$ = 0.3 mm. Since the Bijker model assumes that the bed roughness k_s is equal to max(η,D_{90}), but does not include a procedure for the calculation of the ripple height (η), the procedure outlined earlier for the calculation of ripple dimensions has been implemented *locally* within SISYPHE to estimate the variation of η, and hence k_s throughout the domain. It should be noted that linear wave theory has been used to calculate near-bed velocity amplitudes, based on the wave heights in Figure 4a, throughout the domain. Although this will probably have led to some inaccuracy in η, and hence k_s, within the surf zone, the trends in the results for k_s shown in Figure 5 are as expected.

For normal wave incidence, the ripples at the edge of the model domain (y = 200 m) are predicted to have heights of about 0.06 m. As the water depth decreases and the wave height increases, the ripple height decreases successively to about 0.02 m at y = 120 m, and 0.01 m at y = 160 m (i.e. close to the break point). Thereafter, as the wave height decreases, the ripple height increases rapidly towards the shoreline, where it again reaches values of about 0.06 m. [The decrease in k_s evident in Figure 5 in the immediate vicinity of the shoreline may be anomalous.] The predicted variations in k_s as the waves shoal and then break are evidently very substantial.

For oblique wave incidence, the variations in k_s are initially less pronounced, the ripple height decreasing to only about 0.03 m at y = 120 m due to the behaviour of the waves in the outer region discussed above. However, the generation of the longshore current has a significant effect on the bed forms in this case, with sheet flow conditions ($k_s = D_{90}$) predicted to occur beneath the longshore 'jet' (y = 165-180 m). In the inner surf zone the roughness is again predicted to increase quite sharply.

The impact on the total longshore sand transport rate of the local roughness variations is shown in Figure 6 for the oblique case. Here the predicted longshore transport rates, based upon the roughness variations in Figure 5, are compared with equivalent results from module SISYPHE based upon 'representative' values of the bed roughness (k_s = 0.01, 0.02 and 0.04 m, see Figure 5) that are assumed to be *constant* throughout the model domain. Bijker's sand transport formulation has been used here; it may be noted that somewhat different results would have been obtained had, say, the TKE-model been used for this purpose. The transport rate is halved approximately if local roughness variations are taken into account, compared with the results obtained assuming a uniform roughness. In fact, the cross-shore profiles of

transport rate show relatively little variation with k_s in the cases of uniform roughness. One of the effects of the local variations in k_s is to produce a slight reduction in the transport rate from y = 160 to 165 m as a result of the predicted onset of sheet flow conditions beneath the longshore jet. Maximum transport is predicted at the centre of the jet (y = 175 m), as expected, whatever is assumed for the roughness.

Although the variations in longshore transport rate highlighted in Figure 6 are substantial, they have no particular significance for morphological evolution in the present simple case. However, the results do suggest that, in general cases involving topographic changes (e.g. bars, pits or banks) in the model domain, neglect of local roughness variations may lead to substantial errors in transport rates that may, in turn, affect the morphological outcome when long-duration simulations are made. Work of this kind is presently being undertaken using an extension of the standard version of the SISYPHE module, in order to assess the impact on morphological outcomes of the temporal evolution of the local bed roughness (i.e. k_s variations in space and time). Use of variations in k_s such as those proposed by Van Rijn (1993) (see Table 1) would appear to along the right lines, and to be far preferable to assuming a uniform bed roughness throughout the model domain. However, the differences in the predictions of transport rates between Figures 1 and 2 (prescribed and predicted k_s, respectively) serves to highlight the sensitivity of transport results to the detailed variations of k_s that may occur on site. Moreover, morphological models require robust, easily implemented, and well validated prediction schemes for ripple dimensions, rather than *ad hoc* assumptions based upon the modeller's intuitions. At the present stage of research, there remains a need for improved schemes of this kind.

2.5 Conclusions

In the coastal zone, variations in the bed roughness (k_s) may be substantial as waves shoal and break, and also interact with wave-induced and tidal currents. The associated roughness variations are likely to have a major effect on local sand transport rates throughout the coastal area. This has been demonstrated here by a comparison involving a turbulence-closure TKE-model that has been run over a wide range of wave and current conditions. Initially, for each wave-current condition studied, the bed roughness has been *prescribed* in a qualitatively realistic, but somewhat *ad hoc* manner, leading to a set of predictions for the total sand transport rate. Then, for the same set of conditions, the roughness has been *predicted*, using an approach based on the ripple prediction scheme for waves alone of Wiberg and Harris (1994), moderated by the procedure of Tanaka and Dang (1996) for the superimposition of a current. Using the predicted roughnesses, a rather different set of transport curves is produced by the TKE model. A further comparison over the same range of wave and current conditions has been carried out using Bijker's (1971) sand transport model. This produces significantly different predictions compared with the TKE model, giving insight into the consequences of using different sand transport models.

A comparison involving waves incident on a plane sloping beach has been presented to highlight the expected variation in the bed roughness as waves approach the shoreline. Here the TELEMAC Modelling System has been used to generate the wave field, for the cases of both normal and oblique wave incidence. In the latter case, a strong wave-induced longshore current is generated by the radiation stresses. The predicted cross-shore variations in bed

roughness are very substantial. In the case of oblique wave incidence, the predicted ripple height is 0.06 m well outside the breaker line, while plane bed (sheet flow) conditions are predicted beneath the longshore 'jet' in the outer surf zone. In the inner surf zone, ripples are again predicted to occur, with a consequent increase in the local bed roughness. The net longshore sand transport rate given by the Bijker model for the case of predicted, locally varying bed roughness is about one half of that obtained by use of a representative, constant value of k_s throughout the model domain, highlighting the sensitivity of nearshore sand transport predictions to the choice of bed roughness.

From the point of view of morphological modellers, it is tempting to argue that detailed changes in sand transport rates resulting from *local* roughness variations may have little impact upon the final morphological outcome. However, this proposition needs to be tested for a range of coastal scenarios before it can be accepted. The morphological outcome will depend additionally, of course, on the choice of sand transport model. Fortunately, as demonstrated by Davies et al. (2002), most research and practical sand transport formulations exhibit a similar general behaviour, over a wide range of wave and current conditions, at least when confronted by a prescribed bed roughness. However, if the bed roughness on site is not known, morphological modellers should be conscious of the fact that much uncertainty still exists in respect of sand transport rate predictions, and also that far more robust, validated methods are still required for the prediction of ripple dimensions and, hence, the bed roughness.

2.6 Figures

List of figures:

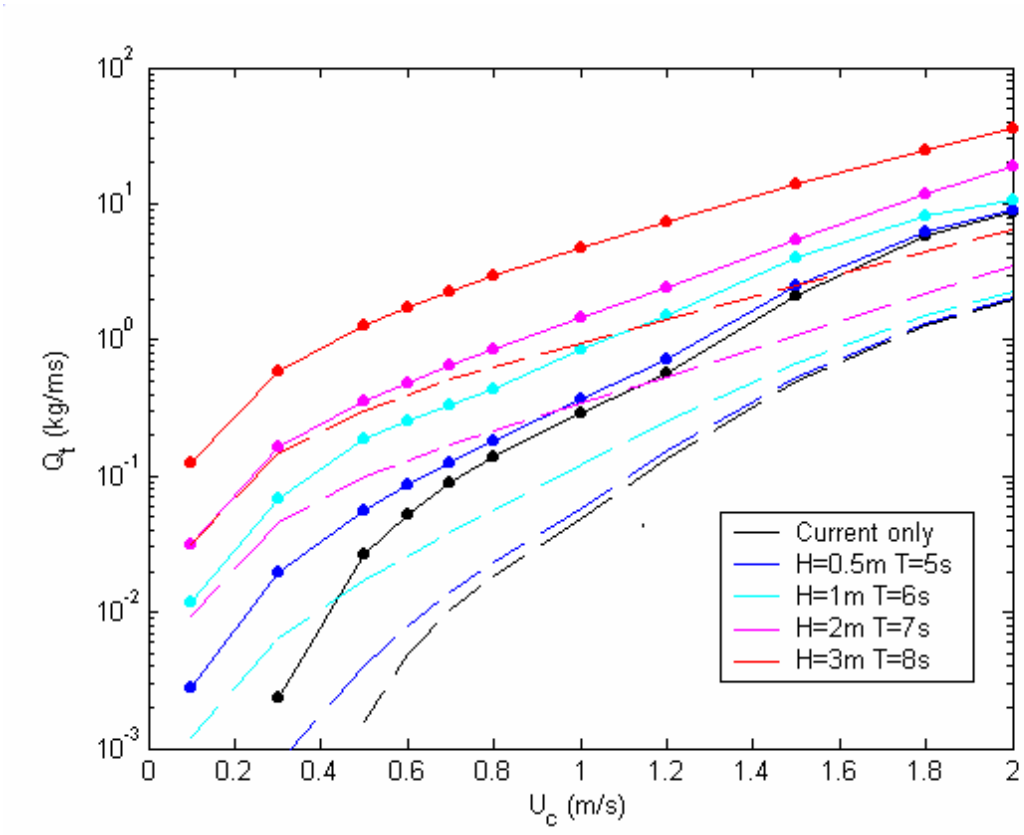

Fig. 1. Total transport rates predicted by the TKE-model with the roughness (k_s) prescribed as in Table 2.

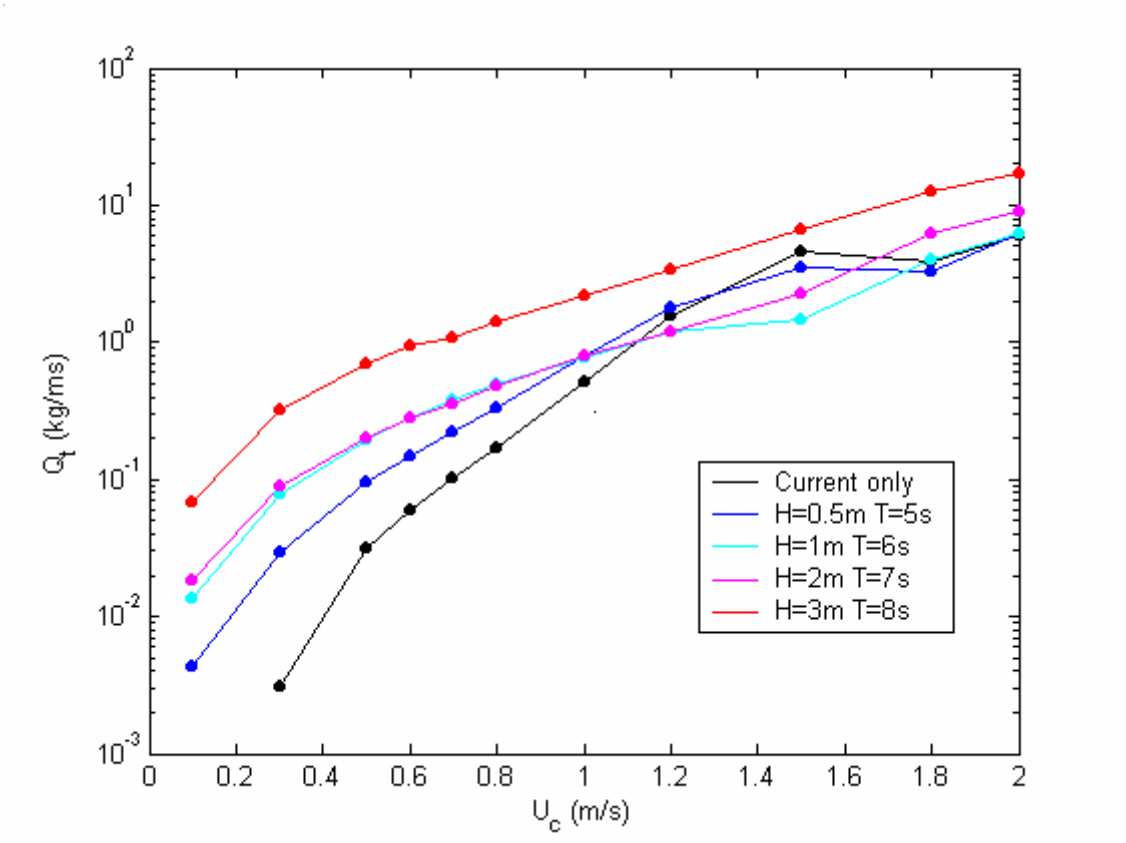

Fig. 2. TKE-model results equivalent to those in Fig.1,but with k_s predicted using the procedure of Davies and Villaret (2000).

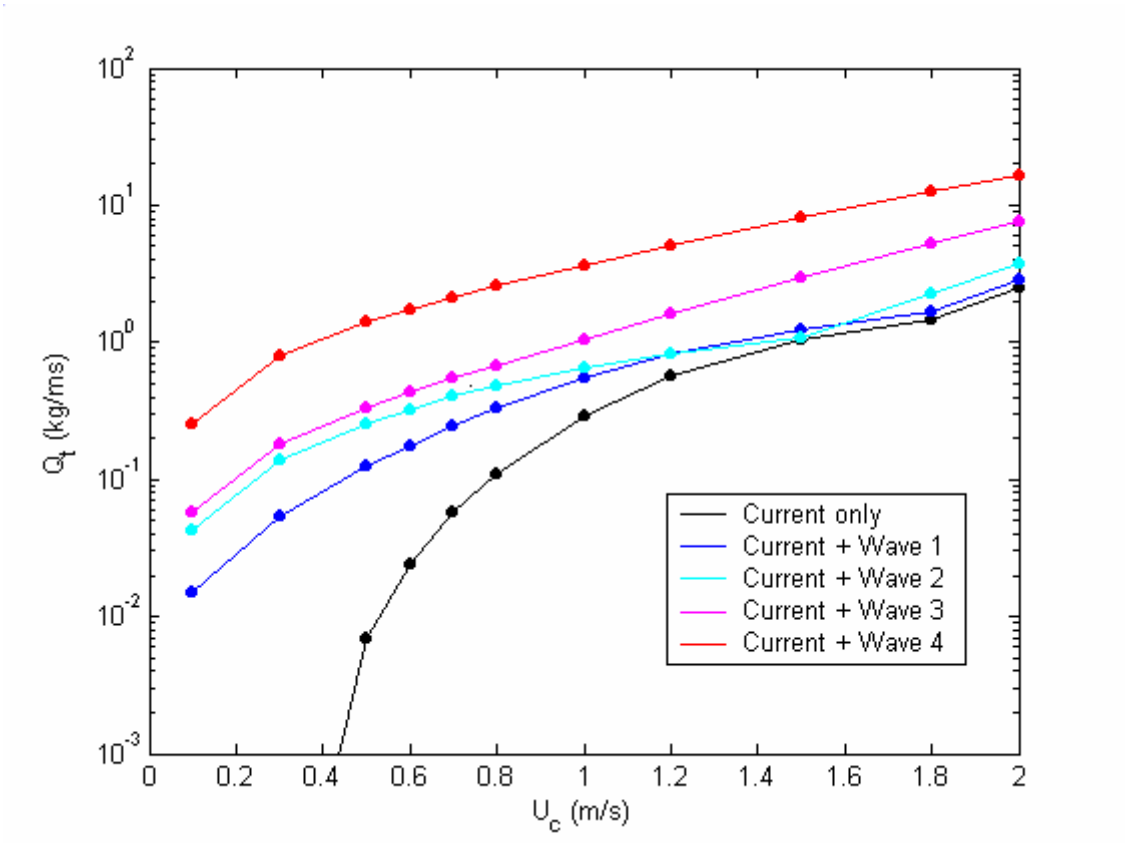

Fig. 3. Results equivalent to those in Fig. 2 based on Bijker's (1991) sand transport model with prescribed values of roughness k_s.

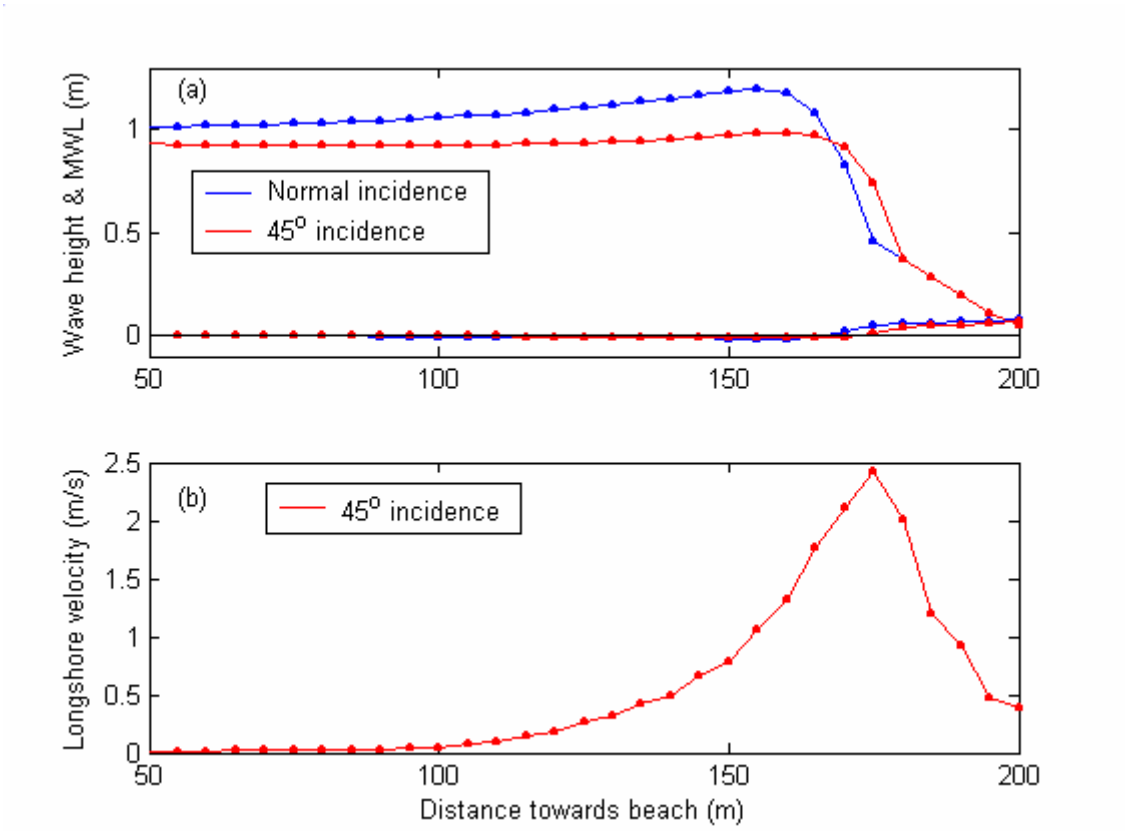

Fig.4. Cross-shore profiles of (a) wave height and mean water level (MWL), and (b) longshore mean velocity.

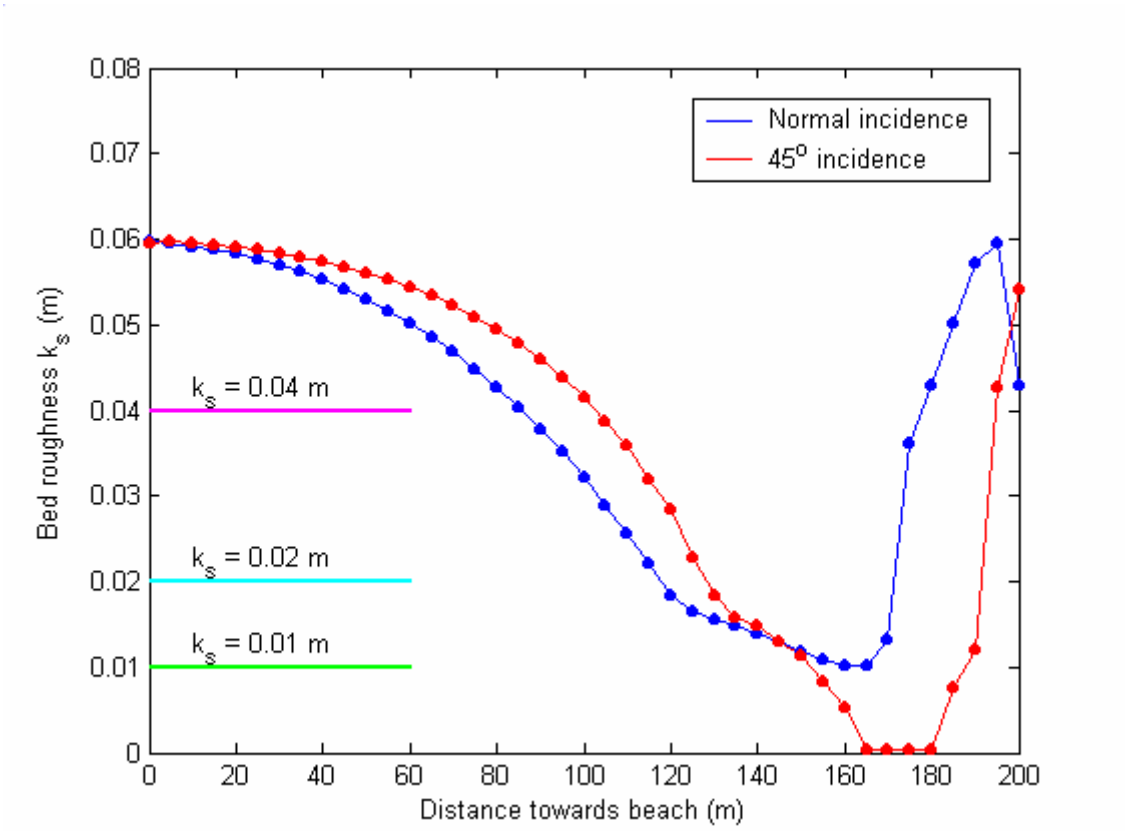

Fig.5. Cross-shore profiles of predicted bed roughness (k_s) for the cases of normal and oblique wave incidence, together with the 3 representative values of k_s used in Figure 6.

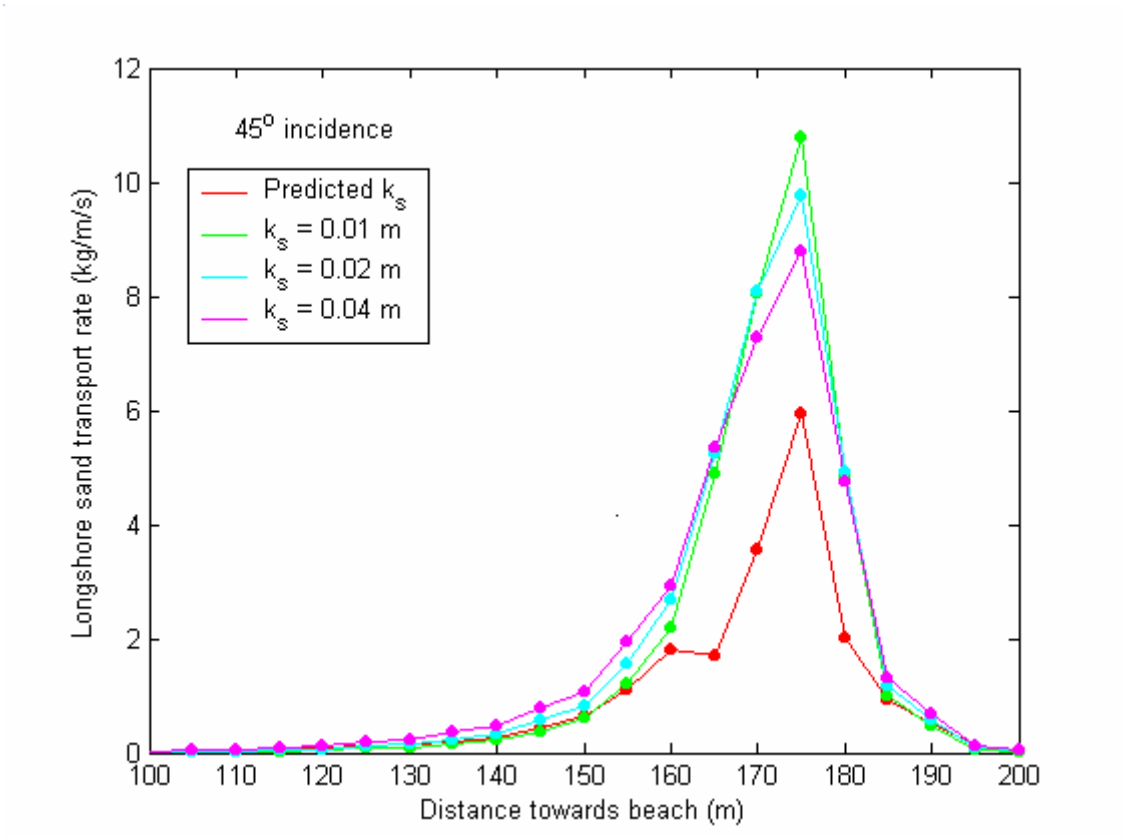

Fig. 6. Cross-shore profiles of total longshore sand transport rate predicted by the Bijker (1971) sand transport model, using the predicted and representative (constant) values of k_s indicated.

2.7 References

Andersen, K.H., and Fredsøe, J. 1999. How to calculate the geometry of vortex ripples. *Proceedings of Coastal Sediments 1999*, Long Island, ASCE, 78-93.

Bijker, E.W., 1971. Longshore transport computations. Journal of Waterways, Harbours and Coastal Engineering Division, American Society of Civil Engineers, 97, WW4, 687-701.

Bijker, E.W., 1992. Mechanics of sediment transport by the combination of waves and current, In Design and Reliability of Coastal Structures, 23rd Int. Conf. on Coastal Engineering, 147-173.

Block, M.E., Davies, A.G., and Villaret, C. 1994. Suspension of sand in oscillatory flow above ripples: discrete vortex model and laboratory experiments. In: Belorgey, M., Rajaona, R.D., Sleath, J.F.A. (Eds.), *Sediment Transport Mechanisms in Coastal Environments and Rivers*, World Scientific, Singapore, 37-52.

Blondeaux, P., and Vittori, G. 1991. Vorticity dynamics in an oscillatory flow over a rippled bed. *Journal of Fluid Mechanics*, 226, 257-289.

Davies, A.G., and Li, Z. 1997. Modelling sediment transport beneath regular symmetrical and asymmetrical waves above a plane bed. *Continental Shelf Research*, 17(5), 555-582.

Davies, A.G., and Thorne, P.D., 2002. 1DV-model of sand transport by waves and currents in the rippled bed regime. *Proceedings of the 28th International Conference on Coastal Engineering*, Cardiff, ASCE. In Press.

Davies, A.G., and Villaret, C. 1997. Oscillatory flow over rippled beds: Boundary layer structure and wave-induced Eulerian drift. In: Hunt, J.N. (Ed.), *Gravity Waves in Water of Finite Depth, Advances in Fluid Mechanics*, Computational Mechanics Publications, Southampton, UK, 215-254.

Davies, A.G., and Villaret, C. 1999. Eulerian drift induced by progressive waves above rippled and very rough beds. *Journal of Geophysical Research*, 104, 1465-1488.

Davies, A.G., and Villaret, C. 2000. Sand transport by waves and currents: predictions of research and engineering models. *Proceedings of the 27th International Conference on Coastal Engineering*, Sydney, ASCE, 2481-2494.

Davies, A.G., and Villaret C. 2002. Prediction of sand transport rates by waves and currents in the coastal zone. *Continental Shelf Research*, In Press.

Davies, A.G., Ribberink, J.S., Temperville, A. & Zyserman, J.A., 1997. Comparisons between sediment transport models and observations made in wave and current flows above plane beds. Coastal Engineering, 31, 163-198.

Davies A.G., Van Rijn L.C., Damgaard J.S., van de Graaff J. and J.S. Ribberink, 2002. Intercomparison of research and practical sand transport models. Coastal Engineering, 46, 1-23.

Fredsøe, J., and Deigaard, R. 1992. *Mechanics of Coastal Sediment Transport*, World Scientific, Singapore, 369pp.

Hansen, E.A., Fredsøe, J., and Deigaard, R. 1994. Distribution of suspended sediment over wave-generated ripples. *Journal of Waterway, Port, Coastal and Ocean Engineering*, 120, 37-55.

Longuet-Higgins, M.S. 1981. Oscillating flow over steep sand ripples. *Journal of Fluid Mechanics*, 107, 1-35.

Malarkey J. and A.G. Davies, 2002. Discrete vortex modelling of oscillatory flow over ripples. Applied Ocean Research, 24, 3, 127-145.

Malarkey, J., Davies, A.G., and Li, Z. 2002. A simple model of oscillatory sheet flow. *Proceedings of the 28th International Conference on Coastal Engineering*, Cardiff, ASCE. In Press.

Malarkey J. and A.G. Davies, 2003. A non-iterative procedure for the Wiberg and Harris (1994) oscillatory sand ripple predictor. Journal of Coastal Research. In Press.

Nielsen, P. 1992. *Coastal bottom boundary layers and sediment transport*, World Scientific Publishing Co., Singapore, 324 pp.

Sleath, J.F.A. 1991. Velocities and shear stresses in wave-current flows. *Journal of Geophysical Research*, 96(C8), 15237-15244.

Swart, D.H. 1976. Offshore sediment transport and equilibrium beach profiles. *Delft Hydraulics Report*, Publ. 131, Delft University, Netherlands.

Tanaka, H., and Dang, V.T. 1996. Geometry of sand ripples due to combined wave-current flows. *Journal of Waterway, Port, Coastal and Ocean Engineering*, 122(6), 298-300.

Van Rijn, L.C., 1973. Principles of sediment transport in rivers, estuaries and coastal seas. Aqua Publications, Amsterdam.

Van Rijn L.C., Davies A.G., van de Graaff J. and J.S. Ribberink (Eds.), 2001. SEDMOC : Sediment Transport Modelling in Marine Coastal Environments. Aqua Publications, Amsterdam, 415pp.

Wiberg, P.L., & Harris, C.K., 1994. Ripple geometry in wave-dominated environments. Journal of Geophysical Research, 99, C1, 775-789.

Wilson, K.C., 1989. Mobile-bed friction at high shear stress. Journal of Hydraulic Engineering, 115, 6, 825-830.

3. APPENDIX

Ripples dimensions can be predicted as a function of wave (orbital velocity U_0 and period $T=2\pi/\omega$), for a given uniform sediment diameter D_{50}, following the procedure of Wiberg and Harris (1994). This formulation is only applicable for oscillatory flow conditions and does not account for the effect of a superimposed mean current.

Ripples can be classified into three types depending on the value of the ratio of wave orbital diameter to mean grain diameter, D_0/D_{50}, where $D_0= 2U_0/\omega$. The ripples dimensions, namely their wave length λ and height η, could be calculated as follows:

In the orbital ripples regime, under moderate wave conditions ($D_0 < D_{cr1}$), ripples dimensions are simply proportional to D_0:

$$\lambda = 0.62 D_0$$
$$\eta = 0.17 \lambda$$

For larger waves, (($D_0 > D_{cr2}$), in the anorbital ripple regime, ripples dimensions scale with the sand grain diameter:

$$\lambda = 535 D_{50}$$
$$\eta = \lambda \exp\left(-0.095 \left(Log \frac{D_0}{\eta} \right)^2 + 0.042 Log \frac{D_0}{\eta} - 2.28 \right)$$

The last equation leads shows that the ripple height progressively decreases as the waves increase to be finally washed out entirely. This equation can be rewritten in the following form

$$X = Log \frac{D_0}{\eta} \quad and \quad Y = Log \frac{D_0}{D_{50}}$$
$$Y = -A X^2 + BX + C$$
$$A = 0.095$$
$$B = 1 + 0.042$$
$$C = 2.28 - Log\, 535$$

We have therefore to solve a second-order equation for a given set of (D_0, D_{50})values:

$$X = \frac{B -/+ \sqrt{B^2 - 4A(C+Y)}}{2A}$$

This equation admits real positive root, if the expression under the square root sign is positive ie :

$$Y < \frac{B^2}{4A} - C$$

Which means that the method can be applied only up to a certain limiting value of D_0/D_{50} (≈ 13020). Above this, ripples are entirely washed out (sheet flow regime).

The delimitation between the different regimes depends on the ration D_0/η_a, where η_a is the anorbital ripples height , as calculated by solving equation:

$$\frac{D_0}{\eta_a} < 20 : orbital$$

$$\frac{D_0}{\eta_a} > 100 : anorbital$$

In the intermediate suborbital regime $20< D_0/\eta_a< 100$, ripples length is calculated as a geometrical average of its anorbital and orbital values:

$$Log\lambda - Log\lambda_a = \frac{Log(D_0/\eta_a) - Log(100)}{Log(20) - Log(100)}(Log\lambda_{orb} - Log\lambda_a)$$

The ripple steepness is the same as in the anorbital regime, and obtained by solving the 2nd order equation as a function of D_0 and D_{50}.

The method can be summarized in the following steps:

1. Calculate the anorbital ripples dimensions
2. Determine the ripple type, from the value of D_0/η_a
3. Calculate D_0/λ
4. Calculate η/λ

Results are plotted on the figure below.

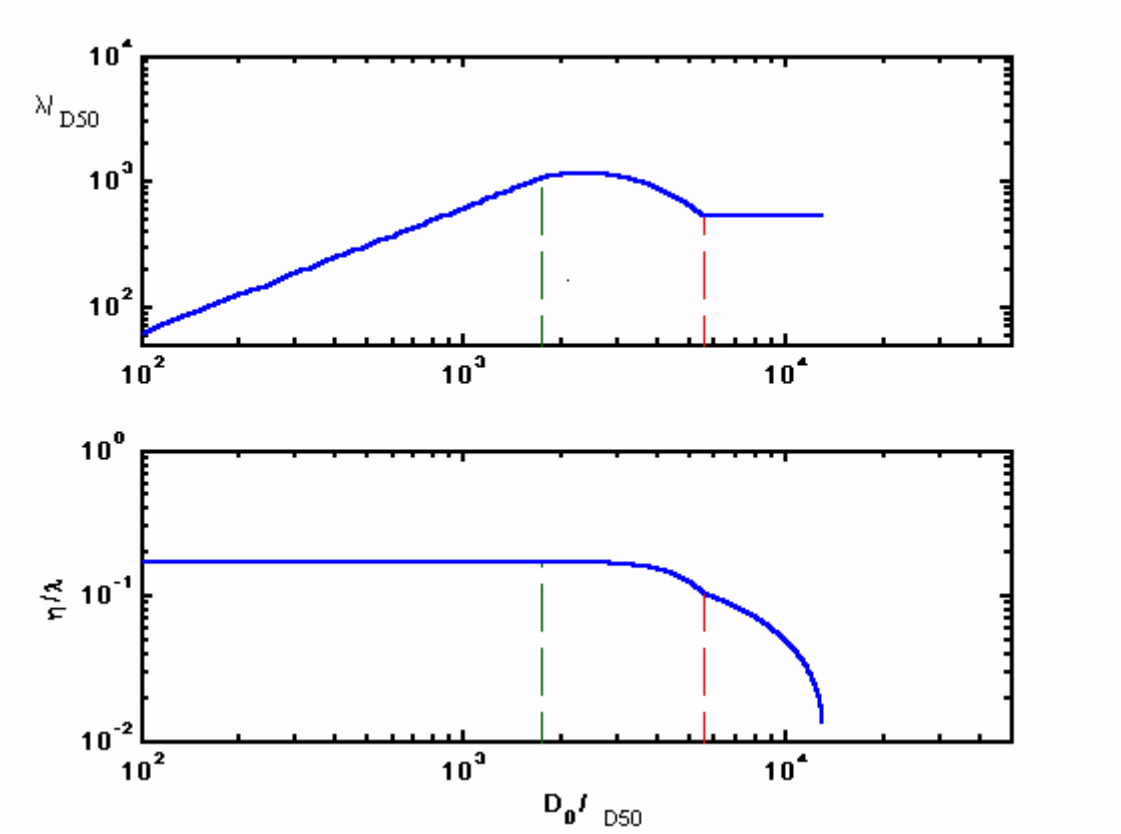

Figure : Dimensions of equilibrium wave-induced ripples based on the method of Wiberg et Harris (1992).